

Adaptive Control of Hyperbolic PDEs Coupled With a Disturbed and Highly Uncertain ODE

Ji Wang , Member, IEEE, Shu-Xia Tang , Senior Member, IEEE, and Miroslav Krstic , Fellow, IEEE

Abstract—In this article, we address adaptive output-feedback boundary control of coupled hyperbolic partial differential equations (PDEs) with spatially varying coefficients and on a time-varying domain, whose uncontrolled boundary is coupled with a disturbed ordinary differential equation (ODE), where multiple parameters in the state matrix and the amplitudes of the harmonic disturbance are unknown. The asymptotic convergence to zero of the ODE state and the boundedness of the PDE states are ensured. This article is motivated by lateral vibration suppression of a mining cable elevator, where the interaction dynamics between the cage and the flexible guide is approximated as a viscoelastic system, including spring and damping, with unknown stiffness and damping coefficients. The performance of the proposed controller is tested in the application of the mining cable elevator by numerical simulation.

Index Terms—Adaptive control, anticollocated disturbance, backstepping, cable elevators, coupled hyperbolic partial differential equations (PDEs).

I. INTRODUCTION

A. Motivation

A mining cable elevator is used to transport a cage loaded with the minerals and miners via cables for thousands of meters between the underground and the surface. The undesirable mechanical vibrations are often caused in the high-speed operation, because of the stretching and contracting abilities of cables. It would not only increase the risk of cable fracture, but also cause discomfort or injury to miners. Active vibration control is one economic way to suppress vibrations because the main structure of the mining elevator does not need to be changed. Because the length of the cable is thousands of meters long and time varying, the infinite dimension and time-varying properties are dominant in the elevator, whose dynamics are described by partial differential equations (PDEs) on the time-varying domain, coupled with an ordinary differential equation (ODE)

Manuscript received 24 October 2020; revised 31 July 2021; accepted 30 November 2021. Date of publication 20 December 2021; date of current version 28 December 2022. Recommended by Associate Editor Martin Guay. (Corresponding author: Shu-Xia Tang.)

Ji Wang is with the Department of Automation, Xiamen University, Xiamen 361005, China (e-mail: jiwang@xmu.edu.cn).

Shu-Xia Tang is with the Department of Mechanical Engineering, Texas Tech University, Lubbock TX 79409 USA (e-mail: shuxia.tang@ttu.edu).

Miroslav Krstic is with the Department of Mechanical and Aerospace Engineering, University of California, San Diego, La Jolla, CA 92093 USA (e-mail: krstic@ucsd.edu).

Color versions of one or more figures in this article are available at <https://doi.org/10.1109/TAC.2021.3136771>.

Digital Object Identifier 10.1109/TAC.2021.3136771

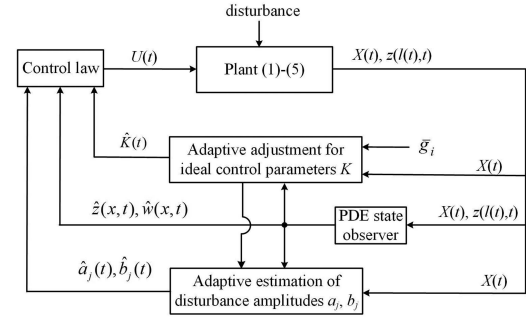


Fig. 1. Block of the closed-loop system.

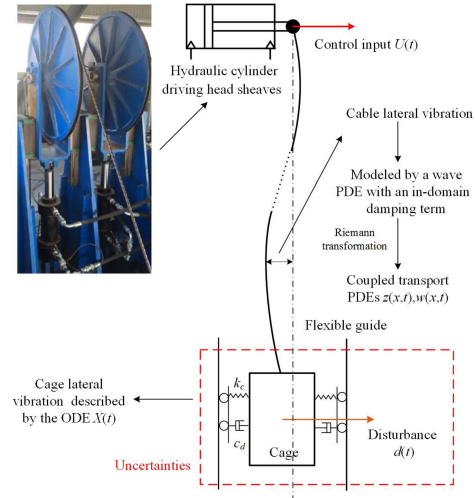


Fig. 2. Lateral vibration control of a mining cable elevator with viscoelastic guides.

describing cage dynamics at the uncontrolled boundary. Based on such a distributed parameter system, some boundary control strategies [25]–[29] were proposed to suppress the axial vibrations of the elevator considering that the actuators and sensors can only be installed at the boundaries of the cable. For the lateral vibrations, an important influencing factor is interaction between the cage and the flexible guides. The elastic support of flexible guides was approximated as a spring–damping system, i.e., a viscoelastic guide [23], [32], where the stiffness and damping coefficients k_c and c_d are difficult to be known exactly (see Fig. 2). It leads to unknown parameters in the state matrix of the ODE describing the cage dynamics at the uncontrolled boundary of the time-varying domain PDE. Moreover, the cage is always subject to uncertain airflow disturbances [31], which

increases the unmatched uncertainties and instabilities in the PDE systems.

The objective is then to design a control law at the top of a vibrational cable with a time-varying length to regulate the cage at the bottom, where the information of interaction between the cage and viscoelastic guides (parameters in the state matrix of the ODE) are unknown, and the cage is subject to uncertain external disturbances. The vibrational cable with material damping is described as coupled transport PDEs converted from wave PDEs with damping terms via Riemann transformations [29].

B. Boundary Control of Coupled Transport PDEs

Many authors have contributed to boundary control of coupled transport PDEs for the past ten years. The basic boundary stabilization problem of 2×2 coupled linear transport PDEs by backstepping was addressed in [8] and [24]. By applying the sliding-mode approach and the proportional-integral controller design, control of such a 2×2 system was also considered in [18] and [22], respectively. Boundary control of the 2×2 transport PDE system was further extended to that of an $n + 1$ system in [12]. For a more general coupled transport PDE system, where the number of PDEs in either direction is arbitrary [16], a boundary stabilization law was first designed by backstepping, which was a systematic framework for the backstepping-based control of this kind of system. Adaptive control for unknown system parameters or disturbance rejection for external periodic disturbances has been further developed in [4]–[6] and [1], [2], [9], [10] respectively. Considering the payload at the bottom of the cable, the plant becomes a coupled transport PDE system coupled with an ODE at the uncontrolled boundary. Boundary control of the type of this system was also studied in [11], [13], and [29]. However, the control problem in lateral vibration suppression of mining cable elevators with viscoelastic guides mentioned in the first paragraph, i.e., boundary control of 2×2 transport PDEs coupled with an ODE at the uncontrolled boundary, where multiple parameters in the state matrix and the amplitudes of the external disturbances in the ODE are unknown, is unsolved and challenging.

C. Contributions

- 1) Based on the boundary control method of coupled hyperbolic PDEs in [11], [13], [16], [28], and [29], we further consider adaptive control of coupled hyperbolic PDEs coupled with a disturbed and highly uncertain ODE anticollocated with the PDE boundary control input, motivated by a practical control problem in the mining cable elevator with a disturbed cage moving along a flexible guide.
- 2) As compared to adaptive control of 2×2 coupled hyperbolic PDEs in [4] and [5], our concern plant is characterized by the time-varying PDE domain and an additional disturbed unstable ODE anticollocated with the control input.
- 3) Different from the disturbance attenuation results in hyperbolic PDEs [10], [31], the concern task in this article requires us to solve the problems of not only the uncertain external disturbances, but also unknown plant parameters.
- 4) Compared with the recent work [30] about adaptive control of a wave PDE–ODE system with an unknown

damping coefficient and a disturbance in the ODE, in addition to the fact that more parameters in the state matrix of the ODE are unknown, this article considers additional couplings and spatially varying coefficients in the time-varying PDE domain, which make control design more challenging because the control input needs to go through the PDE domain to regulate the disturbed and highly uncertain ODE.

This is the first result of boundary control of coupled hyperbolic PDEs, whose uncontrolled boundary is coupled with a disturbed ODE with a state matrix, including multiple unknown parameters. The comparisons with the related results are summarized in Table I.

D. Organization

The rest of this article is organized as follows. The problem formulation is shown in Section II, where the plant is a coupled PDE–ODE system. Under the condition that the ODE state is fully measured, an observer is designed to estimate the PDE states in Section III. The design of the output-feedback controller via the backstepping method is proposed in Section IV. Adaptive update laws for the unknown parameters are given in Section V. In Section VI, the adaptive output-feedback control law is presented and the stability result of the closed-loop control system is proved. Simulation test in a mining cable elevator is provided in Section VII. Finally, Section VIII concludes this article.

II. PROBLEM FORMULATION

The plant concerned in this article is

$$\dot{X}(t) = AX(t) + Bw(0, t) + B_1d(t) \quad (1)$$

$$z(0, t) = CX(t) - p_1w(0, t) \quad (2)$$

$$z_t(x, t) = -q_1(x)z_x(x, t) + c_1(x)z(x, t) + c_2(x)w(x, t) \quad (3)$$

$$w_t(x, t) = q_2(x)w_x(x, t) + c_3(x)z(x, t) + c_4(x)w(x, t) \quad (4)$$

$$w(l(t), t) = U(t) + p_2z(l(t), t) \quad (5)$$

for $x \in [0, l(t)]$, $t \in [0, \infty)$. The vector $X(t) \in \mathbb{R}^n$ is an ODE state, whereas $z(x, t)$ and $w(x, t)$ are transport PDE states. The control input $U(t)$ is to be designed.

Remark 1: The plant (1)–(5) can be used to model the vibration dynamics of the mining cable elevator. As mentioned in Section I-A, the vibration dynamics of the mining cable elevator is originally modeled by a wave PDE–ODE system, where the wave PDE describes the lateral vibration of the cable and the ODE describes that of the cage, and then, it is converted to the coupled hyperbolic PDE–ODE plant (1)–(5) via the Riemann transformation. More details of physical meanings of the plant (1)–(5), the wave PDE-modeled lateral vibration dynamics of the mining cable elevator, and the Riemann transformation are given in Section VII.

In (3) and (4), the spatially varying transport speeds q_1 and q_2 are positive-valued $C^1([0, L])$ functions, and c_1, c_2, c_3 , and c_4 are $C^0([0, L])$ functions, where the positive constant L is the upper bound of $l(t)$, as will be seen in Assumption 3. The constant p_1 is nonzero and the constant p_2 is arbitrary. The matrix $C \in \mathbb{R}^{1 \times n}$ is arbitrary. The matrix $A \in \mathbb{R}^{n \times n}$ is the system

TABLE I
COMPARISONS WITH RECENT AND RELATED RESULTS

	In-domain couplings between hyperbolic PDEs	Unknown plant parameters anti-collocated with control	External disturbances anti-collocated with control	Time-varying domain	Coupled with unstable ODEs
[16]	✓	✗	✗	✗	✗
[13],[11]	✓	✗	✗	✗	✓
[29],[28]	✓	✗	✗	✓	✓
[4],[5]	✓	✓	✗	✗	✗
[2],[10]	✓	✗	✓	✗	✗
[31]	✗	✗	✓	✓	✓
[30]	✗	✓	✓	✗	✓
This paper	✓	✓	✓	✓	✓

✓ means that the content is included in the study and ✗ denotes “not included.”

matrix, and $B \in \mathbb{R}^{n \times 1}$ is the input matrix and $B_1 = Bb_d$, where b_d is an arbitrary constant. The matrices A and B and the signal $d(t)$ are expected to satisfy the following assumptions.

Assumption 1: The matrix A and the vector B are in the form of

$$A = \begin{pmatrix} 0 & 1 & 0 & 0 & \cdots & 0 \\ 0 & 0 & 1 & 0 & \cdots & 0 \\ \vdots & & & & & \\ 0 & 0 & 0 & 0 & \cdots & 1 \\ g_1 & g_2 & g_3 & \cdots & g_{n-1} & g_n \end{pmatrix}, \quad B = \begin{pmatrix} 0 \\ 0 \\ 0 \\ 0 \\ \vdots \\ h_n \end{pmatrix} \quad (6)$$

where the constants $g_1, g_2, g_3, \dots, g_{n-1}, g_n$ are unknown and arbitrary, and their lower and upper bounds are known and arbitrary. The constant h_n is nonzero and known.

Assumption 1 indicates that the ODE is in the controllable form, which covers many practical models, including the cage dynamics considered in this article.

Choosing a target Hurwitz matrix

$$A_m = \begin{pmatrix} 0 & 1 & 0 & 0 & \cdots & 0 \\ 0 & 0 & 1 & 0 & \cdots & 0 \\ \vdots & & & & & \\ 0 & 0 & 0 & 0 & \cdots & 1 \\ \bar{g}_1 & \bar{g}_2 & \bar{g}_3 & \cdots & \bar{g}_{n-1} & \bar{g}_n \end{pmatrix} \quad (7)$$

where the constants $\bar{g}_1, \bar{g}_2, \bar{g}_3, \dots, \bar{g}_{n-1}, \bar{g}_n$ are determined by the users according to the desired performance for the specific application, such as the required stiffness coefficient and damping coefficient in the cage guide dynamics in Fig. 2. According to Assumption 1 and the choice such that the matrix A_m in (7) is Hurwitz, we know that there exists a unique, though unknown, row vector

$$K_{1 \times n} = [k_1, \dots, k_n] \quad (8)$$

such that

$$A_m = A + BK. \quad (9)$$

As a result

$$k_i = \frac{1}{h_n}(\bar{g}_i - g_i), \quad i = 1, 2, \dots, n. \quad (10)$$

By virtue of (10), and given that the lower and upper bounds of the g_i 's are known in Assumption 1, and the \bar{g}_i 's are chosen by the users, while the k_i 's are unknown, the lower and upper bounds on the k_i 's, i.e., $[k_i, \bar{k}_i]$, $i = 1, 2, \dots, n$, are known.

Assumption 2: The disturbance $d(t)$ is of the general harmonic form as $d(t) = \sum_{j=1}^N [a_j \cos(\theta_j t) + b_j \sin(\theta_j t)]$, where the integer N is arbitrary. The frequencies $\theta_j, j \in \{1, 2, \dots, N\}$, are known and arbitrary constants. The amplitudes a_j and b_j are unknown constants bounded by the known and arbitrary positive constants \bar{a}_j and \bar{b}_j in the sense of $|a_j| \in [0, \bar{a}_j]$, $|b_j| \in [0, \bar{b}_j]$.

Assumption 2 can model all periodic disturbance signals to an arbitrarily high degree of accuracy by choosing N sufficiently large.

The time-varying domain $[0, l(t)]$ associated with the moving boundary $l(t)$, which is a known time-varying function, is under the following two assumptions.

Assumption 3: The function $l(t)$ is bounded, i.e., $0 < l(t) \leq L \quad \forall t \geq 0$, where L is a positive constant.

The constant L is the maximal length of the cable in the application of vibration suppression of mining cable elevators.

Assumption 4: The function $\dot{l}(t)$ is bounded as

$$|\dot{l}(t)| < \min_{0 \leq x \leq L} \{q_1(x), q_2(x)\} \quad \forall t \geq 0. \quad (11)$$

As will be seen in Section VII-A, the coupled transport PDEs with the moving boundary can be converted from a wave PDE with the moving boundary via the Riemann transformation. According to the results in [14] and [15], the fact that the speed of the moving boundary is smaller than the wave speed (i.e., the transport speed in the coupled transport PDEs) ensures well-posedness of the initial boundary value problem of the wave PDE with the moving boundary. Therefore, together with invertibility of the Riemann transformation, the limit of the speed of the moving boundary in Assumption 4 ensures the well-posedness of the plant (1)–(5). This assumption holds in the application of the mining cable elevator, as we shall see in Section VII-A.

III. OBSERVER DESIGN

A. Observer Structure and Observer Error System

To estimate the PDE states $(z(x, t), w(x, t))^T$, i.e., the vibration state in the cable, which usually cannot be fully measured in practice but are required in the controller, an observer for the PDE states is designed in this section. The observer states are denoted as $\hat{z}(x, t)$ and $\hat{w}(x, t)$ and define the observer error state as

$$(\tilde{z}(x, t), \tilde{w}(x, t)) = (z(x, t), w(x, t)) - (\hat{z}(x, t), \hat{w}(x, t)). \quad (12)$$

Remark 2: In the mining cable elevator, the ODE state $X(t)$ physically means the vibration displacement and velocity of the cage, which can be obtained by the acceleration sensor placed at the cage plus integral algorithm [25]. Therefore, only estimation of the PDE states is pursued here.

Rewriting $w(0, t)$ in the ODE (1) as the sum of the observer state $\hat{w}(0, t)$ and the observer error $\tilde{w}(0, t)$, i.e., $w(0, t) = \hat{w}(0, t) + \tilde{w}(0, t)$, yields

$$\dot{X}(t) = AX(t) + B\hat{w}(0, t) + B\tilde{w}(0, t) + B_1d(t). \quad (13)$$

Using the measurements $X(t), z(l(t), t)$, the observer for the PDE states is built as

$$\hat{z}(0, t) = CX(t) - p_1\hat{w}(0, t) \quad (14)$$

$$\begin{aligned} \hat{z}_t(x, t) = & -q_1(x)\hat{z}_x(x, t) + c_1(x)\hat{z}(x, t) + c_2(x)\hat{w}(x, t) \\ & + \Phi_2(x, t)(z(l(t), t) - \hat{z}(l(t), t)) \end{aligned} \quad (15)$$

$$\begin{aligned} \hat{w}_t(x, t) = & q_2(x)\hat{w}_x(x, t) + c_3(x)\hat{z}(x, t) + c_4(x)\hat{w}(x, t) \\ & + \Phi_3(x, t)(z(l(t), t) - \hat{z}(l(t), t)) \end{aligned} \quad (16)$$

$$\hat{w}(l(t), t) = U(t) + p_2z(l(t), t) \quad (17)$$

where the functions $\Phi_2(x, t)$ and $\Phi_3(x, t)$ are observer gains to be determined. According to (2)–(5) and (14)–(17), recalling (12), the observer error system is obtained as

$$\tilde{z}(0, t) = -p_1\tilde{w}(0, t) \quad (18)$$

$$\begin{aligned} \tilde{z}_t(x, t) = & -q_1(x)\tilde{z}_x(x, t) + c_1(x)\tilde{z}(x, t) + c_2(x)\tilde{w}(x, t) \\ & - \Phi_2(x, t)\tilde{z}(l(t), t) \end{aligned} \quad (19)$$

$$\begin{aligned} \tilde{w}_t(x, t) = & q_2(x)\tilde{w}_x(x, t) + c_3(x)\tilde{z}(x, t) + c_4(x)\tilde{w}(x, t) \\ & - \Phi_3(x, t)\tilde{z}(l(t), t) \end{aligned} \quad (20)$$

$$\tilde{w}(l(t), t) = 0. \quad (21)$$

Observer gains $\Phi_2(x, t)$ and $\Phi_3(x, t)$ are to be designed to ensure convergence to zero of the observer errors.

B. Determining Observer Gains via Backstepping

Postulate the invertible backstepping transformation

$$\begin{aligned} \tilde{z}(x, t) = & \tilde{\alpha}(x, t) - \int_x^{l(t)} \bar{\phi}(x, y)\tilde{\alpha}(y, t)dy \\ & - \int_x^{l(t)} \check{\phi}(x, y)\tilde{\beta}(y, t)dy \end{aligned} \quad (22)$$

$$\begin{aligned} \tilde{w}(x, t) = & \tilde{\beta}(x, t) - \int_x^{l(t)} \bar{\psi}(x, y)\tilde{\alpha}(y, t)dy \\ & - \int_x^{l(t)} \check{\psi}(x, y)\tilde{\beta}(y, t)dy \end{aligned} \quad (23)$$

to convert the original observer error system (18)–(21) to the following target observer error systems:

$$\tilde{\alpha}(0, t) = -p_1\tilde{\beta}(0, t) \quad (24)$$

$$\tilde{\alpha}_t(x, t) = -q_1(x)\tilde{\alpha}_x(x, t) + c_1(x)\tilde{\alpha}(x, t) \quad (25)$$

$$\tilde{\beta}_t(x, t) = q_2(x)\tilde{\beta}_x(x, t) + c_4(x)\tilde{\beta}(x, t) \quad (26)$$

$$\tilde{\beta}(l(t), t) = 0. \quad (27)$$

The form of the backstepping transformation (22), (23) for coupled hyperbolic PDEs is taken from [16], which also proves the invertibility of the backstepping transformation. The integration interval chosen in the transformation (22), (23) is $[x, l(t)]$ because the PDE boundary measurement used in the observer is at the boundary $x = l(t)$. Even though the integration interval is time varying, the kernels in (22) and (23) need not include the time argument because the extra terms introduced by the time-varying integration interval during the calculation of the kernel conditions will be “absorbed” by the time-dependent observer gains $\Phi_2(x, t)$ and $\Phi_3(x, t)$, which will be seen clearly later.

By matching (18)–(21) and (24)–(27) using (22) and (23) (the details are shown in Appendix A), the conditions on the kernels $\bar{\phi}(x, y), \bar{\psi}(x, y), \check{\phi}(x, y), \check{\psi}(x, y)$ in (22) and (23) are obtained as the following two well-posed hyperbolic systems:

$$\begin{aligned} q_2(x)\bar{\psi}_x(x, y) - q_1(y)\bar{\psi}_y(x, y) \\ = - (c_4(x) - c_1(y) - q_1'(y))\bar{\psi}(x, y) - c_3(x)\bar{\phi}(x, y) \end{aligned} \quad (28)$$

$$\begin{aligned} -q_1(x)\bar{\phi}_x(x, y) - q_1(y)\bar{\phi}_y(x, y) \\ = - (c_1(x) - c_1(y) - q_1'(y))\bar{\phi}(x, y) - c_2(x)\bar{\psi}(x, y) \end{aligned} \quad (29)$$

$$\bar{\psi}(x, x) = \frac{-c_3(x)}{q_1(x) + q_2(x)} \quad (30)$$

$$\bar{\phi}(0, y) = -p_1\bar{\psi}(0, y) \quad (31)$$

and

$$\begin{aligned} q_2(x)\check{\psi}_x(x, y) + q_2(y)\check{\psi}_y(x, y) \\ = - (c_4(x) - c_4(y) + q_2'(y))\check{\psi}(x, y) - c_3(x)\check{\phi}(x, y) \end{aligned} \quad (32)$$

$$\begin{aligned} -q_1(x)\check{\phi}_x(x, y) + q_2(y)\check{\phi}_y(x, y) \\ = - (c_1(x) - c_4(y) + q_2'(y))\check{\phi}(x, y) - c_2(x)\check{\psi}(x, y) \end{aligned} \quad (33)$$

$$\check{\phi}(x, x) = \frac{c_2(x)}{q_1(x) + q_2(x)} \quad (34)$$

$$\check{\psi}(0, y) = -\frac{1}{p_1}\check{\phi}(0, y) \quad (35)$$

on $\mathcal{D}(t) = \{0 \leq x \leq y \leq l(t)\}$. The observer gains are, thus, determined as

$$\Phi_2(x, t) = \dot{l}(t)\bar{\phi}(x, l(t)) - q_1(l(t))\bar{\phi}(x, l(t)) \quad (36)$$

$$\Phi_3(x, t) = \dot{l}(t)\bar{\psi}(x, l(t)) - q_1(l(t))\bar{\psi}(x, l(t)). \quad (37)$$

Remark 3: Equations (28)–(31) and (32)–(35), are in the same form with the kernel equations (24)–(31) in [24], if we extend the time-varying triangular domain $\mathcal{D}(t)$ to a fixed triangular domain $\mathcal{D}_1 = \{0 \leq x \leq y \leq L\}$ (L is defined in Assumption 3). Because the boundary conditions in (28)–(31) and (32)–(35) on the triangular domain $\mathcal{D}(t)$ are given along the lines $y = x$ and $x = 0$ rather than on $y = l(t)$, it is feasible to extend the domain $\mathcal{D}(t)$ to the fixed triangular domain \mathcal{D}_1 when solving (28)–(31) and (32)–(35). That is, the solutions of (28)–(31) and (32)–(35) on $\mathcal{D}(t)$ can be obtained by solving (28)–(31) and (32)–(35) on \mathcal{D}_1 whose well-posedness is proved in [24]. This ensures the existence of the observer gains $\Phi_2(x, t)$ and $\Phi_3(x, t)$ in (36) and (37), consisting of $\bar{\phi}(x, l(t))$ and $\bar{\psi}(x, l(t))$ obtained by extracting the results along $y = l(t)$ in the solution of (28)–(31) on \mathcal{D}_1 , and the bounded $\dot{l}(t)$ in Assumption 4.

C. Stability of the Observer Error System

Lemma 1: For all initial data $(\tilde{z}(\cdot, 0), \tilde{w}(\cdot, 0)) \in H^1(0, L)$, the states $\tilde{z}(\cdot, t)$ and $\tilde{w}(\cdot, t)$ of the observer error system (18)–(21) with the observer gains (36), (37) become and remain zero no later than the time $t = t_a$, where $t_a = \frac{L}{\min_{0 \leq x \leq L} \{q_1(x)\}} + \frac{L}{\min_{0 \leq x \leq L} \{q_2(x)\}}$.

Proof: According to the target observer error system (24)–(27) and the result in [16], we know that $\tilde{\alpha}(x, t)$ and $\tilde{\beta}(x, t)$ reach zero by the time t_a , at the latest. Applying the Cauchy–Schwarz inequality into (22) and (23), the proof of this lemma is complete.

Remark 4: For the application of the mining cable elevators, Lemma 1 physically means that the designed observer (14)–(17), which uses only boundary measurements, can effectively recover the actual distributed states of the vibrating string.

IV. ADAPTIVE DISTURBANCE CANCELLATION AND STABILIZATION

In this section, we design an observer-based output-feedback controller. We conduct the state-feedback control design based on the observer using the backstepping method, which makes the resulting control law employ only the observer states. Three transformations are used to convert the observer (13)–(17) to a target system, with the intention of adaptively canceling the unmatched disturbance (the disturbance at the cage), removing the coupling in the PDE domain, and making the system matrix of the ODE Hurwitz (stabilizing the vibrating cable and cage in the application of the mining cable elevators).

The output injection signals $\tilde{z}(l(t), t)$ and $\tilde{w}(0, t)$ in the observer are regarded as zero in the control design, following which the separation principle, which is verified by the fact that the observer errors $\tilde{z}(x, t), \tilde{w}(x, t)$ vanish in finite time only depending on the plant parameters according to Lemma 1, is applied in the stability analysis of the resulting output-feedback closed-loop system.

A. First Transformation for Adaptively Canceling the Unmatched Disturbance

Defining

$$Z(t) = [\cos(\theta_1 t), \sin(\theta_1 t), \dots, \cos(\theta_N t), \sin(\theta_N t)]^T \quad (38)$$

where the superscript T means transposition, we then have

$$\dot{Z}(t) = A_z Z(t) \quad (39)$$

where

$$A_z = \text{diag} \left[\left(\begin{array}{cc} 0 & -\theta_1 \\ \theta_1 & 0 \end{array} \right), \dots, \left(\begin{array}{cc} 0 & -\theta_N \\ \theta_N & 0 \end{array} \right) \right]. \quad (40)$$

According to Assumption 2, the disturbance can be written as $d(t) = [a_1, b_1, \dots, a_N, b_N]Z(t)$. Define the disturbance estimate $\hat{d}(t)$ as

$$\hat{d}(t) = [\hat{a}_1(t), \hat{b}_1(t), \dots, \hat{a}_N(t), \hat{b}_N(t)]Z(t) \quad (41)$$

where $\hat{a}_1(t), \hat{b}_1(t), \dots, \hat{a}_N(t), \hat{b}_N(t)$ are estimates of $a_1, b_1, \dots, a_N, b_N$, which will be shown in Section V.

We then introduce the transformation $(\hat{w}, \hat{z}) \rightarrow (\hat{v}, \hat{s})$

$$\hat{v}(x, t) = \hat{w}(x, t) + \Gamma(x, t)Z(t) \quad (42)$$

$$\hat{s}(x, t) = \hat{z}(x, t) + \Gamma_1(x, t)Z(t) \quad (43)$$

where $\Gamma(x, t)$ and $\Gamma_1(x, t)$ are to be determined, to convert (13)–(17) into the following system:

$$\dot{X}(t) = AX(t) + B\hat{v}(0, t) + B_1\tilde{d}(t) \quad (44)$$

$$\hat{s}(0, t) + p_1\hat{v}(0, t) = CX(t) \quad (45)$$

$$\begin{aligned} \hat{s}_t(x, t) = & -q_1(x)\hat{s}_x(x, t) + c_1(x)\hat{s}(x, t) + c_2(x)\hat{v}(x, t) \\ & + \Gamma_{1t}(x, t)Z(t) \end{aligned} \quad (46)$$

$$\hat{v}_t(x, t) = q_2(x)\hat{v}_x(x, t) + c_3(x)\hat{s}(x, t) + c_4(x)\hat{v}(x, t)$$

$$+ \Gamma_t(x, t)Z(t) \quad (47)$$

$$\begin{aligned} \hat{v}(l(t), t) = & U(t) + p_2\hat{s}(l(t), t) \\ & + (\Gamma(l(t), t) - p_2\Gamma_1(l(t), t))Z(t) \end{aligned} \quad (48)$$

where $\tilde{d}(t)$ is given as

$$\begin{aligned} \tilde{d}(t) = & d(t) - \hat{d}(t) \\ = & \sum_{j=1}^N [(a_j - \hat{a}_j(t)) \cos(\theta_j t) + (b_j - \hat{b}_j(t)) \sin(\theta_j t)] \\ = & \sum_{j=1}^N [\tilde{a}_j(t) \cos(\theta_j t) + \tilde{b}_j(t) \sin(\theta_j t)]. \end{aligned} \quad (49)$$

The functions $\Gamma(x, t)$ and $\Gamma_1(x, t)$ in (42) and (43) are determined as follows. Taking the time and spatial derivatives of (42) and (43) and substituting the result into (46) and (47), recalling (15), (16), and (39), we get

$$\begin{aligned} & \hat{s}_t(x, t) + q_1(x)\hat{s}_x(x, t) - c_1(x)\hat{s}(x, t) \\ & - c_2(x)\hat{v}(x, t) - \Gamma_{1t}(x, t)Z(t) \\ = & \hat{z}_t(x, t) + q_1(x)\hat{z}_x(x, t) + \Gamma_{1t}(x, t)Z(t) + \Gamma_1(x, t)A_z Z(t) \\ & - c_2(x)\hat{w}(x, t) - c_1(x)\hat{z}(x, t) + q_1(x)\Gamma_{1x}(x, t)Z(t) \\ & - c_2(x)\Gamma(x, t)Z(t) - c_1(x)\Gamma_1(x, t)Z(t) - \Gamma_{1t}(x, t)Z(t) \\ = & (\Gamma_1(x, t)A_z + q_1(x)\Gamma_{1x}(x, t) \\ & - c_2(x)\Gamma(x, t) - c_1(x)\Gamma_1(x, t))Z(t) = 0 \end{aligned} \quad (50)$$

$$\begin{aligned} & \hat{v}_t(x, t) - q_2(x)\hat{v}_x(x, t) - c_3(x)\hat{s}(x, t) \\ & - c_4(x)\hat{v}(x, t) - \Gamma_t(x, t)Z(t) \\ = & \hat{w}_t(x, t) - q_2(x)\hat{w}_x(x, t) + \Gamma_t(x, t)Z(t) + \Gamma(x, t)A_z Z(t) \\ & - c_4(x)\hat{w}(x, t) - c_3(x)\hat{z}(x, t) - q_2(x)\Gamma_x(x, t)Z(t) \\ & - c_4(x)\Gamma(x, t)Z(t) - c_3(x)\Gamma_1(x, t)Z(t) - \Gamma_t(x, t)Z(t) \\ = & (\Gamma(x, t)A_z - q_2(x)\Gamma_x(x, t) \\ & - c_4(x)\Gamma(x, t) - c_3(x)\Gamma_1(x, t))Z(t) = 0. \end{aligned} \quad (51)$$

For (50) and (51) to hold, we obtain the conditions

$$\begin{aligned} & -q_2(x)\Gamma_x(x, t) + \Gamma(x, t)(A_z - c_4(x)I_{2N}) \\ & - c_3(x)\Gamma_1(x, t) = 0 \end{aligned} \quad (52)$$

$$\begin{aligned} & q_1(x)\Gamma_{1x}(x, t) + \Gamma_1(x, t)(A_z - c_1(x)I_{2N}) \\ & - c_2(x)\Gamma(x, t) = 0 \end{aligned} \quad (53)$$

where I_{2N} is an identity matrix with dimension $2N$.

Defining $\zeta(x, t) = [\Gamma(x, t), \Gamma_1(x, t)]$, then (52) and (53) are rewritten as

$$\zeta_x(x, t) = -\zeta(x, t)\bar{A}(x) \quad (54)$$

where

$$\begin{aligned} \bar{A}(x) = & \begin{pmatrix} A_z - c_4(x)I_{2N} & -c_2(x)I_{2N} \\ -c_3(x)I_{2N} & A_z - c_1(x)I_{2N} \end{pmatrix} \\ & \times \begin{pmatrix} -q_2(x)I_{2N} & 0_{2N} \\ 0_{2N} & q_1(x)I_{2N} \end{pmatrix}^{-1}. \end{aligned}$$

By mapping (13), (14) and (44), (45) through the transformation (42), (43), recalling (41) and $B_1 = Bb_d$, we obtain the condition

$$\begin{aligned}\zeta(0, t) &= [\Gamma(0, t), \Gamma_1(0, t)] \\ &= b_d[\hat{a}_1(t), \hat{b}_1(t), \dots, \hat{a}_N(t), \hat{b}_N(t), \\ &\quad -p_1\hat{a}_1(t), -p_1\hat{b}_1(t), \dots, -p_1\hat{a}_N(t), -p_1\hat{b}_N(t)].\end{aligned}\quad (55)$$

The solution to (54) and (55) is

$$\zeta(x, t) = \zeta(0, t)\bar{H}(x) \quad (56)$$

where $\bar{H}(x)$ is the unique solution of the following initial value problem:

$$\bar{H}_x(x) = -\bar{H}(x)\bar{\mathcal{A}}(x), \bar{H}(0) = I_{4N} \quad (57)$$

for $x \in [0, L]$.

B. Second Transformation for Decoupling PDEs

We postulate the backstepping transformation

$$\begin{aligned}\hat{\beta}(x, t) &= \hat{v}(x, t) - \int_0^x \bar{\vartheta}(x, y)\hat{s}(y, t)dy \\ &\quad - \int_0^x \check{\vartheta}(x, y)\hat{v}(y, t)dy\end{aligned}\quad (58)$$

$$\begin{aligned}\hat{\alpha}(x, t) &= \hat{s}(x, t) - \int_0^x \bar{\lambda}(x, y)\hat{s}(y, t)dy \\ &\quad - \int_0^x \check{\lambda}(x, y)\hat{v}(y, t)dy\end{aligned}\quad (59)$$

to convert (44)–(48) into the following system:

$$\dot{X}(t) = AX(t) + B\hat{\beta}(0, t) + B_1\tilde{d}(t) \quad (60)$$

$$\hat{\alpha}(0, t) = CX(t) - p_1\hat{\beta}(0, t) \quad (61)$$

$$\begin{aligned}\hat{\alpha}_t(x, t) &= -q_1(x)\hat{\alpha}_x(x, t) + c_1(x)\hat{\alpha}(x, t) \\ &\quad - \bar{\lambda}(x, 0)q_1(0)CX(t) \\ &\quad + \left(\Gamma_{1t}(x, t) - \int_0^x \bar{\lambda}(x, y)\Gamma_{1t}(y, t)dy \right. \\ &\quad \left. - \int_0^x \check{\lambda}(x, y)\Gamma_t(y, t)dy \right) Z(t)\end{aligned}\quad (62)$$

$$\begin{aligned}\hat{\beta}_t(x, t) &= q_2(x)\hat{\beta}_x(x, t) + c_4(x)\hat{\beta}(x, t) \\ &\quad - \bar{\vartheta}(x, 0)q_1(0)CX(t) \\ &\quad - \left(\int_0^x \check{\vartheta}(x, y)\Gamma_t(y, t)dy \right. \\ &\quad \left. + \int_0^x \bar{\vartheta}(x, y)\Gamma_{1t}(y, t)dy - \Gamma_t(x, t) \right) Z(t)\end{aligned}\quad (63)$$

$$\begin{aligned}\hat{\beta}(l(t), t) &= U(t) + p_2\hat{s}(l(t), t) \\ &\quad + (\Gamma(l(t), t) - p_2\Gamma_1(l(t), t))Z(t) \\ &\quad - \int_0^{l(t)} \bar{\vartheta}(l(t), y)\hat{s}(y, t)dy \\ &\quad - \int_0^{l(t)} \check{\vartheta}(l(t), y)\hat{v}(y, t)dy.\end{aligned}\quad (64)$$

By matching (60)–(64) and (44)–(48) via (58) and (59) (the details are shown in Appendix B), the conditions of kernels $\bar{\lambda}(x, y)$, $\check{\lambda}(x, y)$, $\bar{\vartheta}(x, y)$, $\check{\vartheta}(x, y)$ are obtained as the following two well-posed hyperbolic systems:

$$\begin{aligned}&-q_1(x)\check{\lambda}_x(x, y) + q_2(y)\check{\lambda}_y(x, y) \\ &= -(q_2'(y) + c_1(x) - c_4(y))\bar{\lambda}(x, y) + c_2(y)\bar{\lambda}(x, y)\end{aligned}\quad (65)$$

$$\begin{aligned}q_1(x)\bar{\lambda}_x(x, y) + q_1(y)\bar{\lambda}_y(x, y) \\ = -(q_1'(y) + c_1(y) - c_1(x))\bar{\lambda}(x, y) - c_3(y)\check{\lambda}(x, y)\end{aligned}\quad (66)$$

$$\check{\lambda}(x, x) = \frac{c_2(x)}{q_1(x) + q_2(x)} \quad (67)$$

$$\bar{\lambda}(x, 0) = -\frac{q_2(0)}{q_1(0)p_1}\check{\lambda}(x, 0) \quad (68)$$

and

$$\begin{aligned}q_2(x)\check{\vartheta}_x(x, y) + q_2(y)\check{\vartheta}_y(x, y) \\ = -(q_2'(y) + c_4(x) - c_4(y))\check{\vartheta}(x, y) \\ + c_2(y)\bar{\vartheta}(x, y)\end{aligned}\quad (69)$$

$$\begin{aligned}-q_2(x)\bar{\vartheta}_x(x, y) + q_1(y)\bar{\vartheta}_y(x, y) \\ = -(q_1'(y) + c_1(y) - c_4(x))\bar{\vartheta}(x, y) \\ - c_3(y)\check{\vartheta}(x, y)\end{aligned}\quad (70)$$

$$\bar{\vartheta}(x, x) = -\frac{c_3(x)}{q_1(x) + q_2(x)} \quad (71)$$

$$\check{\vartheta}(x, 0) = -\frac{q_1(0)p_1}{q_2(0)}\bar{\vartheta}(x, 0) \quad (72)$$

on $\{0 \leq y \leq x \leq l(t)\}$. The equation sets (65)–(68) and (69)–(72) are in the same form as (28)–(31) and (32)–(35). One can refer to Remark 3 and [24] for the well-posedness of (65)–(68) and (69)–(72).

C. Third Transformation for a Stable ODE

We postulate the backstepping transformation

$$\begin{aligned}\hat{\eta}(x, t) &= \hat{\beta}(x, t) - \int_0^x \hat{N}(x, y; \hat{K}(t))\hat{\beta}(y, t)dy \\ &\quad - D(x; \hat{K}(t))X(t)\end{aligned}\quad (73)$$

where the update law for $\hat{K}(t) \in \mathbb{R}^{1 \times n}$ is developed in the next section. The conditions for the kernels $\hat{N}(x, y; \hat{K}(t))$ and $D(x; \hat{K}(t))$ are to be determined later. The inverse transformation is defined as

$$\begin{aligned}\hat{\beta}(x, t) &= \hat{\eta}(x, t) - \int_0^x \hat{N}^I(x, y; \hat{K}(t))\hat{\eta}(y, t)dy \\ &\quad - D^I(x; \hat{K}(t))X(t)\end{aligned}\quad (74)$$

where \hat{N}^I and D^I are the kernels whose existence and continuity will be shown later.

Through the transformation (73), we convert (60)–(64) into the following target system:

$$\dot{X}(t) = A_m X(t) + B\hat{\eta}(0, t) + B_1\tilde{d}(t) - B\tilde{K}(t)X(t) \quad (75)$$

$$\hat{\alpha}(0, t) = (C - p_1D(0; \hat{K}(t)))X(t) - p_1\hat{\eta}(0, t) \quad (76)$$

$$\begin{aligned}\hat{\alpha}_t(x, t) &= -q_1(x)\hat{\alpha}_x(x, t) + c_1(x)\hat{\alpha}(x, t) \\ &\quad - \bar{\lambda}(x, 0)q_1(0)CX(t) \\ &\quad + \left(\Gamma_{1t}(x, t) - \int_0^x \bar{\lambda}(x, y)\Gamma_{1t}(y, t)dy \right.\end{aligned}$$

$$\begin{aligned}
& - \int_0^x \check{\lambda}(x, y) \Gamma_t(y, t) dy \Big) Z(t) \\
\hat{\eta}_t(x, t) &= q_2(x) \hat{\eta}_x(x, t) + c_4(x) \hat{\eta}(x, t) \\
& + \left[\Gamma_t(x, t) - \int_0^x \check{\vartheta}(x, y) \Gamma_t(y, t) dy \right. \\
& - \int_0^x \bar{\vartheta}(x, y) \Gamma_{1t}(y, t) dy \\
& - \int_0^x \hat{N}(x, y; \hat{K}(t)) \left(- \int_0^y \check{\vartheta}(y, z) \Gamma_t(z, t) dz \right. \\
& \left. \left. - \int_0^y \bar{\vartheta}(y, z) \Gamma_{1t}(z, t) dz + \Gamma_t(y, t) \right) dy \right] Z(t) \\
& + \left(D(x; \hat{K}(t)) B \tilde{K}(t) - \dot{\hat{K}}(t) D_{\hat{K}(t)}(x; \hat{K}(t)) \right) \\
& \times X(t) - \dot{\hat{K}}(t) R(x, t) - D(x; \hat{K}(t)) B_1 \tilde{d}(t) \tag{78}
\end{aligned}$$

$$\hat{\eta}(l(t), t) = 0 \tag{79}$$

where

$$\tilde{K}(t) = K - \hat{K}(t) \tag{80}$$

and where

$$\begin{aligned}
R(x, t) &= \int_0^x \hat{N}_{\hat{K}(t)}(x, y; \hat{K}(t)) \hat{\beta}(y, t) dy \\
&= \int_0^x \hat{N}_{\hat{K}(t)}(x, y; \hat{K}(t)) \left[\hat{\eta}(y, t) \right. \\
&\quad \left. - \int_0^y \hat{N}^I(y, \sigma; \hat{K}(t)) \hat{\eta}(\sigma, t) d\sigma \right. \\
&\quad \left. - D^I(y; \hat{K}(t)) X(t) \right] dy \tag{81}
\end{aligned}$$

with defining $D_{\hat{K}(t)}(x; \hat{K}(t)) = \frac{\partial D(x; \hat{K}(t))}{\partial \hat{K}(t)}$ and $\hat{N}_{\hat{K}(t)}(x, y; \hat{K}(t)) = \frac{\partial \hat{N}(x, y; \hat{K}(t))}{\partial \hat{K}(t)}$.

By matching (60)–(64) and (75)–(79) with the aid of (73) (the details are shown in Appendix C), the conditions on the kernels $N(x, y; \hat{K}(t))$ and $D(x; \hat{K}(t))$ in (73) are determined as follows:

$$D(0; \hat{K}(t)) = \hat{K}(t) \tag{82}$$

$$\begin{aligned}
& - q_2(x) D'(x; \hat{K}(t)) + D(x; \hat{K}(t)) (A_m - c_4(x) - B \hat{K}(t)) \\
& + \bar{\vartheta}(x, 0) q_1(0) C - \int_0^x \hat{N}(x, y; \hat{K}(t)) \bar{\vartheta}(y, 0) q_1(0) C dy = 0 \tag{83}
\end{aligned}$$

$$q_2(y) \hat{N}_y(x, y; \hat{K}(t)) + q_2(x) \hat{N}_x(x, y; \hat{K}(t))$$

$$+ q_2'(y) \hat{N}(x, y; \hat{K}(t)) = 0 \tag{84}$$

$$q_2(0) \hat{N}(x, 0; \hat{K}(t)) - D(x; \hat{K}(t)) B = 0. \tag{85}$$

The equation set (82)–(85) is a transport PDE–ODE coupled system consisting of the transport PDE (84) with the boundary condition (85) on $\{(x, y) | 0 \leq y \leq x \leq l(t)\}$ and the ODE (83) with the initial value (82) on $\{0 \leq x \leq l(t)\}$. It should be noted that $\hat{K}(t)$ is a parameter rather than a variable in the transport

PDE (84), (85) with respect to the independent variables x and y and in the ODE (82), (83) with respect to the independent variable x when solving (82)–(85).

To establish well-posedness of (82)–(85), the transport PDE state $\hat{N}(x, y; \hat{K}(t))$ can be written as a function of its boundary value $D(x; \hat{K}(t))B$. Substituting the result into ODE (83) to replace $\hat{N}(x, y; \hat{K}(t))$, the solution of the ODE $\dot{D}(x; \hat{K}(t))$ can be obtained. The well-posedness of the transport PDE $\hat{N}(x, y; \hat{K}(t))$ (84), (85) is, thus, obtained because of the well-defined boundary condition (85).

The existence and continuity of the kernels \hat{N}^I and D^I in the inverse transformation (74) are shown as follows. Rewrite (73) as

$$\begin{aligned}
\hat{\eta}(x, t) + D(x; \hat{K}(t)) X(t) &= \hat{\beta}(x, t) \\
- \int_0^x \hat{N}(x, y; \hat{K}(t)) \hat{\beta}(y, t) dy. \tag{86}
\end{aligned}$$

Because $\hat{N}(x, y; \hat{K}(t))$ is continuous, according to [21], there exists a unique continuous $\varrho(x, y; \hat{K}(t))$ on $\{(x, y) | 0 \leq x \leq y \leq l(t)\}$ such that

$$\begin{aligned}
\hat{\beta}(x, t) &= \hat{\eta}(x, t) + D(x; \hat{K}(t)) X(t) \\
&+ \int_0^x \varrho(x, y; \hat{K}(t)) (\hat{\eta}(y, t) + D(y; \hat{K}(t)) X(t)) dy \\
&= \hat{\eta}(x, t) + \int_0^x \varrho(x, y; \hat{K}(t)) \hat{\eta}(y, t) dy \\
&+ \left(\int_0^x \varrho(x, y; \hat{K}(t)) D(y; \hat{K}(t)) dy \right. \\
&\quad \left. + D(x; \hat{K}(t)) \right) X(t). \tag{87}
\end{aligned}$$

Comparing (87) and the inverse transformation (74), we obtain the existence and continuity of the kernels $\hat{N}^I(x, y; \hat{K}(t))$, $D^I(x; \hat{K}(t))$.

Finally, for (79) to hold, recalling (73) and (64), we derive the boundary control input $U(t)$, for which the expression is shown in Section VI.

V. ADAPTIVE UPDATE LAWS

Using normalization and projection operators to guarantee boundedness, as is typical in adaptive control designs, the adaptive update laws for self-tuned control gains

$$\hat{K}(t) = [\hat{k}_1(t), \dots, \hat{k}_n(t)] \tag{88}$$

and for the unknown parameters $\hat{a}_j(t)$, $\hat{b}_j(t)$, $j \in \{1, \dots, N\}$, are built as

$$\dot{\hat{k}}_i(t) = \text{Proj}_{[\bar{k}_i, \bar{k}_i]} (\tau_i(t), \hat{k}_i(t)) \tag{89}$$

$$\dot{\hat{a}}_j(t) = \text{Proj}_{[-\bar{a}_j, \bar{a}_j]} (\tau_{1j}(t), \hat{a}_j(t)) \tag{90}$$

$$\dot{\hat{b}}_j(t) = \text{Proj}_{[-\bar{b}_j, \bar{b}_j]} (\tau_{2j}(t), \hat{b}_j(t)) \tag{91}$$

for $i \in \{1, \dots, n\}$, $j \in \{1, \dots, N\}$. For any constants m, M satisfying $m \leq M$ and any r, p , $\text{Proj}_{[m, M]}$ is the standard projection operator given by

$$\text{Proj}_{[m, M]}(r, p) = \begin{cases} 0, & \text{if } p = m \text{ and } r < 0 \\ 0, & \text{if } p = M \text{ and } r > 0 \\ r, & \text{else.} \end{cases}$$

The role of the projection operator is to keep the parameter estimates bounded. The bounds $\underline{k}_i, \bar{k}_i$ and \bar{a}_j, \bar{b}_j are defined in Section II. The functions τ_i, τ_{1j} , and τ_{2j} in (89)–(91) are defined as

$$[\tau_1(t), \dots, \tau_n(t)]^T = \frac{-\gamma_c (2X B^T P X - r_a \int_0^{l(t)} e^{\delta x} \hat{\eta}(x, t) X B^T D(x; \hat{K}(t))^T dx)}{1 + \Omega(t)} \quad (92)$$

$$\tau_{1j}(t) = \frac{\gamma_{aj} (2X^T P B_1 - r_a \int_0^{l(t)} e^{\delta x} \hat{\eta}(x, t) D(x; \hat{K}(t)) B_1 dx) \cos(\theta_j t)}{1 + \Omega(t)} \quad (93)$$

$$\tau_{2j}(t) = \frac{\gamma_{bj} (2X^T P B_1 - r_a \int_0^{l(t)} e^{\delta x} \hat{\eta}(x, t) D(x; \hat{K}(t)) B_1 dx) \sin(\theta_j t)}{1 + \Omega(t)} \quad (94)$$

where $\Gamma_c = \text{diag}\{\gamma_{c1}, \dots, \gamma_{cn}\}$. The positive update gains γ_{ci} , γ_{aj} , and γ_{bj} are to be chosen by the users, and

$$\delta > \max \left\{ \frac{2\bar{c}_4 + \bar{q}_2'}{q_2}, \frac{2\bar{c}_1 + 1 + \bar{q}_1'}{q_1} \right\} \quad (95)$$

with $\underline{q}_1 = \min_{0 \leq x \leq L} \{q_1(x)\}$, $\bar{q}_1' = \max_{0 \leq x \leq L} \{|q_1'(x)|\}$, $\underline{q}_2 = \min_{0 \leq x \leq L} \{q_2(x)\}$, $\bar{q}_2' = \max_{0 \leq x \leq L} \{|q_2'(x)|\}$, $\bar{c}_1 = \max_{0 \leq x \leq L} \{|c_1(x)|\}$, and $\bar{c}_4 = \max_{0 \leq x \leq L} \{|c_4(x)|\}$.

The scalar functional $\Omega(t)$ is defined as

$$\Omega(t) = X(t)^T P X(t) + \frac{1}{2} r_a \int_0^{l(t)} e^{\delta x} \hat{\eta}(x, t)^2 dx + \frac{1}{2} r_b \int_0^{l(t)} e^{-\delta x} \hat{\alpha}(x, t)^2 dx. \quad (96)$$

The determination of positive constants r_a and r_b will be shown in the next section. The matrix $P = P^T > 0$ is the unique solution to the following Lyapunov equation $P A_m + A_m^T P = -Q$ for some $Q = Q^T > 0$. Because A_m in (7) is known (chosen by the users, in spite of A and K being unknown), the matrix P is known.

The normalization $1 + \Omega(t)$ is introduced in the denominator in (92)–(94) to limit the rates of change of the parameter estimates, i.e., $\hat{k}_i(t)$ and $\hat{a}_j(t), \hat{b}_j(t)$. The functions $\hat{\eta}(\cdot, t)$ and $\hat{\alpha}(\cdot, t)$ in (92)–(94) and (96) can be represented by the observer states through (42), (43), (58), (59), and (73). The idea of constructing the adaptive update laws $\hat{k}_i(t), \hat{a}_j(t), \hat{b}_j(t)$ $i \in \{1, \dots, n\}$, $j \in \{1, \dots, N\}$ in (89)–(94) will be clear from the Lyapunov analysis in Section VI.

VI. CONTROL LAW AND STABILITY ANALYSIS

A. Control Law

According to (64), (73), and (79), $U(t)$ is obtained as

$$U(t) = -p_2 \hat{s}(l(t), t) - (\Gamma(l(t), t) - p_2 \Gamma_1(l(t), t)) Z(t)$$

$$+ \int_0^{l(t)} \bar{\vartheta}(l(t), y) \hat{s}(y, t) dy + \int_0^{l(t)} \check{\vartheta}(l(t), y) \hat{v}(y, t) dy \\ + \int_0^{l(t)} \hat{N}(l(t), y; \hat{K}(t)) \hat{\beta}(y, t) dy \\ + D(l(t); \hat{K}(t)) X(t). \quad (97)$$

Recalling (17), (42), (43), (58), and (73), the control law (97) is rewritten as

$$U(t) = -p_2 z(l(t), t) - \Gamma(l(t), t) Z(t) \\ + \int_0^{l(t)} \bar{\vartheta}(l(t), y) (\hat{z}(y, t) + \Gamma_1(y, t) Z(t)) dy \\ + \int_0^{l(t)} \check{\vartheta}(l(t), y) (\hat{w}(y, t) + \Gamma(y, t) Z(t)) dy \\ + \int_0^{l(t)} \hat{N}(l(t), y; \hat{K}(t)) [\hat{w}(y, t) + \Gamma(y, t) Z(t) \\ - \int_0^y \bar{\vartheta}(y, \sigma) (\hat{z}(\sigma, t) + \Gamma_1(\sigma, t) Z(t)) d\sigma \\ - \int_0^y \check{\vartheta}(y, \sigma) (\hat{w}(\sigma, t) + \Gamma(\sigma, t) Z(t)) d\sigma] dy \\ + D(l(t); \hat{K}(t)) X(t) \quad (98)$$

which is the output-feedback adaptive controller sought in this article. The signals $z(l(t), t)$ and $X(t)$ are measurements and $Z(t)$ is defined in (38). The states $\hat{z}(x, t)$ and $\hat{w}(x, t)$ are obtained from the observer (14)–(17). The functions $\Gamma_1(y, t)$ and $\Gamma(y, t)$ are solutions of (56) and (57), where the adaptive estimates $\hat{a}_j(t)$ and $\hat{b}_j(t)$ are defined in (90), (91), (93), and (94). The functions $\bar{\vartheta}(y, \sigma)$ and $\check{\vartheta}(y, \sigma)$ are solutions of (69)–(72). The functions $\Gamma(l(t), t), \bar{\vartheta}(l(t), y), \check{\vartheta}(l(t), y), \hat{N}(l(t), y; \hat{K}(t))$, and $D(l(t); \hat{K}(t))$ are the solutions of (56), (57), (69)–(72), and (82)–(85) on $x = l(t)$, respectively. The adaptive estimate $\hat{K}(t)$ is defined in (89) and (92).

The block diagram of the closed-loop system is shown in Fig. 1, whose stability result is given in the next subsection.

B. Stability Analysis

The stability analysis of the state-feedback loop is given in the following lemma.

Lemma 2: For all initial data $(\hat{\alpha}(\cdot, 0), \hat{\eta}(\cdot, 0)) \in H^1(0, L)$, $X(0) \in \mathbb{R}^n$, $\hat{K}(0) \in \mathbb{R}^{1 \times n}$, $\hat{a}_j(0) \in \mathbb{R}$, $\hat{b}_j(0) \in \mathbb{R}$, $j = 1, \dots, N$, the target system (75)–(79) is asymptotically regulated in the sense of $\lim_{t \rightarrow \infty} (\|\hat{\alpha}(\cdot, t)\| + \|\hat{\eta}(\cdot, t)\| + |X(t)|) = 0$, where $\|\cdot\|$ denotes the L_2 norm and $|\cdot|$ denotes the Euclidean norm.

Proof: Define

$$\Theta(t) = \|\hat{\eta}(\cdot, t)\|^2 + \|\hat{\alpha}(\cdot, t)\|^2 + |X(t)|^2. \quad (99)$$

Recalling (96), we get $\mu_1 \Theta(t) \leq \Omega(t) \leq \mu_2 \Theta(t)$, where $\mu_1 = \frac{1}{2} \min\{r_a, r_b e^{-\delta L}, \lambda_{\min}(P)\} > 0$, $\mu_2 = \frac{1}{2} \min\{r_a e^{\delta L}, r_b, \lambda_{\max}(P)\} > 0$, and λ_{\min} and λ_{\max} denote the minimum and maximum eigenvalues of the corresponding

matrix. Let us choose a Lyapunov functional as

$$V(t) = \ln(1 + \Omega(t)) + \sum_{j=1}^N \frac{1}{2\gamma_{aj}} \tilde{a}_j(t)^2 + \sum_{j=1}^N \frac{1}{2\gamma_{bj}} \tilde{b}_j(t)^2 + \frac{1}{2} \tilde{K}(t) \Gamma_c^{-1} \tilde{K}(t)^T \quad (100)$$

where \tilde{a}_j , \tilde{b}_j , and \tilde{K} are given in (49) and (80).

Recalling (96), we rewrite the Lyapunov functional as

$$\begin{aligned} V(t) = & \ln \left(X^T P X(t) + \frac{1}{2} r_a \int_0^{l(t)} e^{\delta x} \hat{\eta}(x, t)^2 dx \right. \\ & + \frac{1}{2} r_b \int_0^{l(t)} e^{-\delta x} \hat{\alpha}(x, t)^2 dx + 1 \left. \right) + \sum_{j=1}^N \frac{1}{2\gamma_{aj}} \tilde{a}_j(t)^2 \\ & + \sum_{j=1}^N \frac{1}{2\gamma_{bj}} \tilde{b}_j(t)^2 + \frac{1}{2} \tilde{K}(t) \Gamma_c^{-1} \tilde{K}(t)^T. \end{aligned} \quad (101)$$

Taking the derivative of $V(t)$, through a lengthy calculation in Appendix D, we obtain

$$\begin{aligned} \dot{V}(t) \leq & \frac{1}{1 + \Omega(t)} \left[- \left(\frac{3}{4} \lambda_{\min}(Q) - q_1(0) r_b \bar{d}^2 \right. \right. \\ & - \frac{q_1(0)^2}{2} L r_b \bar{f}^2 |C|^2 \left. \right) |X(t)|^2 \\ & - \left(\frac{1}{2} q_2(0) r_a - q_1(0) r_b p_1^2 - \frac{8}{\lambda_{\min}(Q)} |P B|^2 \right) \hat{\eta}(0, t)^2 \\ & - \left(\frac{1}{2} \underline{q}_2 r_a - r_a \bar{c}_4 - \frac{1}{2} r_a \bar{q}'_2 \right) \int_0^{l(t)} e^{\delta x} \hat{\eta}(x, t)^2 dx \\ & - \frac{1}{2} \left(q_1(l(t)) - \dot{l}(t) \right) r_b e^{-\delta L} \hat{\alpha}(l(t), t)^2 \\ & - \left(\frac{1}{2} \underline{q}_1 \delta r_b - r_b \bar{c}_1 - \frac{1}{2} r_b - \frac{1}{2} r_b \bar{q}'_1 \right) \int_0^{l(t)} e^{-\delta x} \hat{\alpha}(x, t)^2 dx \Big] \\ & - \tilde{K}(t) \left[\Gamma_c^{-1} \dot{\tilde{K}}(t)^T \right. \\ & \left. + \frac{(2 X B^T P X - r_a \int_0^{l(t)} e^{\delta x} \hat{\eta}(x, t) X B^T D(x; \tilde{K}(t))^T dx)}{1 + \Omega(t)} \right] \\ & - \sum_{j=1}^N \tilde{a}_j(t) \left[\frac{1}{\gamma_{aj}} \dot{\tilde{a}}_j(t) \right. \\ & \left. - \frac{(2 X^T P B_1 - r_a \int_0^{l(t)} e^{\delta x} \hat{\eta}(x, t) D(x; \tilde{K}(t)) B_1 dx) \cos(\theta_j t)}{1 + \Omega(t)} \right] \\ & - \sum_{j=1}^N \tilde{b}_j(t) \left[\frac{1}{\gamma_{bj}} \dot{\tilde{b}}_j(t) \right. \\ & \left. - \frac{(2 X^T P B_1 - r_a \int_0^{l(t)} e^{\delta x} \hat{\eta}(x, t) D(x; \tilde{K}(t)) B_1 dx) \sin(\theta_j t)}{1 + \Omega(t)} \right] \\ & + \left[r_a \int_0^{l(t)} e^{\delta x} \hat{\eta}(x, t) (H_b Z(t) - \dot{\tilde{K}}(D_{\tilde{K}} X(t) + R(x, t))) dx \right. \\ & \left. + r_b \int_0^{l(t)} e^{-\delta x} \hat{\alpha}(x, t) H_a Z(t) dx \right] \frac{1}{1 + \Omega(t)}. \end{aligned} \quad (102)$$

Regarding (89)–(91), we know that there exist positive constants m_2 and m_3 such that

$$\begin{aligned} & \max_{j \in \{1, \dots, N\}} \left\{ |\dot{\tilde{a}}_j(t)|^2, |\dot{\tilde{b}}_j(t)|^2 \right\} \\ & \leq m_2 \max_{j \in \{1, \dots, N\}} \{ \gamma_{aj}^2, \gamma_{bj}^2 \} (|X(t)|^2 + \|\hat{\eta}\|^2) \end{aligned} \quad (103)$$

$$|\dot{\tilde{K}}(t)|^2 \leq m_3 \max_{i \in \{1, \dots, n\}} \{ \gamma_{ci}^2 \} \quad (104)$$

where m_2 and m_3 only depend on parameters of the plant and coefficients introduced in the Lyapunov functional.

With (56), we obtain

$$\begin{aligned} & \max_{(x, t) \in [0, L] \times [0, \infty)} \{ |\Gamma_t(x, t)|^2, |\Gamma_{1t}(x, t)|^2 \} \\ & \leq 2N \max_{j \in \{1, \dots, N\}} \left\{ |\dot{\tilde{a}}_j(t)|^2, |\dot{\tilde{b}}_j(t)|^2 \right\} \bar{h}_m^2 \\ & \leq 2N m_2 \max_{j \in \{1, \dots, N\}} \{ \gamma_{aj}^2, \gamma_{bj}^2 \} (|X(t)|^2 + \|\hat{\eta}\|^2) \bar{h}_m^2 \end{aligned} \quad (105)$$

where \bar{h}_m is defined as $\bar{h}_m = \max_{0 \leq x \leq L} \{ \bar{\sigma}(\bar{H}(x)) \}$, and $\bar{H}(x)$ is the solution of (57) and $\bar{\sigma}$ stands for the largest singular value at x .

According to the definitions of H_a and H_b in (D1) and (D2), recalling (104) and (105), there exist positive constants ξ_1 and ξ_2 such that for any $t > 0$,

$$\begin{aligned} & \max \{ |H_a Z(t)|^2, |H_b Z(t)|^2 \} \\ & \leq \xi_1 \max_{j \in \{1, \dots, N\}} \{ \gamma_{aj}^2, \gamma_{bj}^2 \} (|X(t)|^2 + \|\hat{\eta}\|^2) \end{aligned} \quad (106)$$

$$|\dot{\tilde{K}} D_{\tilde{K}(t)} X(t)|^2 \leq \xi_2 \max_{i \in \{1, \dots, n\}} \{ \gamma_{ci}^2 \} |X(t)|^2 \quad (107)$$

with ξ_1 and ξ_2 only depending on the kernels, the parameters of the plant, and the coefficients used in the Lyapunov analysis, but not on γ_{ci} , γ_{aj} , and γ_{bj} .

Applying the Young and Cauchy–Schwarz inequalities, we obtain the inequality

$$\begin{aligned} r_a \int_0^{l(t)} e^{\delta x} \hat{\eta}(x, t) H_b Z(t) dx & \leq \frac{1}{2} r_a \int_0^{l(t)} e^{\delta x} \hat{\eta}(x, t)^2 dx \\ & + \frac{1}{2} r_a e^{\delta L} L \xi_1 \max_{j \in \{1, \dots, N\}} \{ \gamma_{aj}^2, \gamma_{bj}^2 \} (|X(t)|^2 + \|\hat{\eta}\|^2) \end{aligned} \quad (108)$$

where we have used (106), the inequality

$$\begin{aligned} & - r_a \int_0^{l(t)} e^{\delta x} \hat{\eta}(x, t) \dot{\tilde{K}} D_{\tilde{K}(t)} X(t) dx \\ & \leq \frac{r_a}{2} \int_0^{l(t)} e^{\delta x} \hat{\eta}(x, t)^2 dx + \frac{r_a}{2} e^{\delta L} L \max_{i \in \{1, \dots, n\}} \{ \gamma_{ci}^2 \} \xi_2 |X(t)|^2 \end{aligned} \quad (109)$$

where we have used (107), and the inequality

$$\begin{aligned} & - r_a \int_0^{l(t)} e^{\delta x} \hat{\eta}(x, t) \dot{\tilde{K}} R(x, t) dx \leq \frac{1}{2} r_a \int_0^{l(t)} e^{\delta x} \hat{\eta}(x, t)^2 dx \\ & + \frac{1}{2} r_a e^{\delta L} m_3 \max_{i \in \{1, \dots, n\}} \{ \gamma_{ci}^2 \} \xi_3 (|X(t)|^2 + \|\hat{\eta}\|^2) \end{aligned} \quad (110)$$

for which we have employed (81) and (104). The positive constant ξ_3 in (110) only depends on kernels \hat{N}^I , D^I , $\hat{N}_{\tilde{K}(t)}$. Finally, we also obtain the inequality

$$r_b \int_0^{l(t)} e^{-\delta x} \hat{\alpha}(x, t) H_a Z(t) dx \leq \frac{r_b}{2} \int_0^{l(t)} e^{-\delta x} \hat{\alpha}(x, t)^2 dx$$

$$+ \frac{1}{2} r_b L \xi_1 \max_{j \in \{1, \dots, N\}} \{\gamma_{aj}^2, \gamma_{bj}^2\} (|X(t)|^2 + \|\hat{\eta}\|^2) \quad (111)$$

by applying (106). Applying (108)–(111), we obtain

$$\begin{aligned} & r_a \int_0^{l(t)} e^{\delta x} \hat{\eta}(x, t) \left(H_b Z(t) - \dot{\hat{K}} D_{\hat{K}(t)} X(t) - \dot{\hat{K}} R(x, t) \right) dx \\ & + r_b \int_0^{l(t)} e^{-\delta x} \hat{\alpha}(x, t) H_a Z(t) dx \\ & \leq \left[\frac{r_a}{2} e^{\delta L} L \max_{i \in \{1, \dots, n\}} \{\gamma_{ci}^2\} \xi_2 + \frac{r_a}{2} e^{\delta L} L \xi_1 \max_{j \in \{1, \dots, N\}} \{\gamma_{aj}^2, \gamma_{bj}^2\} \right. \\ & \quad \left. + \frac{1}{2} r_a e^{\delta L} m_3 \max_{i \in \{1, \dots, n\}} \{\gamma_{ci}^2\} \xi_3 L \right. \\ & \quad \left. + \frac{1}{2} r_b L \xi_1 \max_{j \in \{1, \dots, N\}} \{\gamma_{aj}^2, \gamma_{bj}^2\} \right] |X(t)|^2 \\ & \quad + \left[\frac{3}{2} r_a e^{\delta L} + \frac{1}{2} r_a e^{\delta L} L \xi_1 \max_{j \in \{1, \dots, N\}} \{\gamma_{aj}^2, \gamma_{bj}^2\} \right. \\ & \quad \left. + \frac{1}{2} r_a e^{\delta L} m_3 \max_{i \in \{1, \dots, n\}} \{\gamma_{ci}^2\} \xi_3 L \right. \\ & \quad \left. + \frac{1}{2} r_b L \xi_1 \max_{j \in \{1, \dots, N\}} \{\gamma_{aj}^2, \gamma_{bj}^2\} \right] \|\hat{\eta}\|^2 + \frac{r_b}{2} \|\hat{\alpha}\|^2 \\ & \leq \max_{i \in \{1, \dots, n\}, j \in \{1, \dots, N\}} \{\gamma_{ci}^2, \gamma_{aj}^2, \gamma_{bj}^2\} \lambda_b \\ & \quad \times (|X(t)|^2 + \|\hat{\eta}\|^2 + \|\hat{\alpha}\|^2) \end{aligned} \quad (112)$$

where $\lambda_b > 0$ only depends on the kernels, the parameters of the plant, and the coefficients used in the Lyapunov analysis.

Choosing

$$r_b < \frac{\frac{3}{4} \lambda_{\min}(Q)}{q_1(0) |\bar{d}|^2 + \frac{q_1(0)^2}{2} L \bar{f}^2 |C|^2} \quad (113)$$

$$r_a > \frac{2}{q_2(0)} \left(q_1(0) r_b p_1^2 - \frac{8}{\lambda_{\min}(Q)} |PB|^2 \right) \quad (114)$$

inserting (112), recalling (95), and applying the adaptive laws (89)–(94), inequality (102) becomes

$$\begin{aligned} \dot{V}(t) & \leq \frac{1}{1 + \Omega} \left[-\lambda_a \left(|X(t)|^2 + \hat{\eta}(0, t)^2 + \|\hat{\eta}(\cdot, t)\|^2 \right. \right. \\ & \quad \left. \left. + \hat{\alpha}(l(t), t)^2 + \|\hat{\alpha}(\cdot, t)\|^2 \right) \right. \\ & \quad \left. + \max_{i \in \{1, \dots, n\}, j \in \{1, \dots, N\}} \{\gamma_{ci}^2, \gamma_{aj}^2, \gamma_{bj}^2\} \lambda_b \left(|X(t)|^2 \right. \right. \\ & \quad \left. \left. + \|\hat{\eta}(\cdot, t)\|^2 + \|\hat{\alpha}(\cdot, t)\|^2 \right) \right]. \end{aligned}$$

The coefficients γ_{aj} , γ_{bj} , and γ_{ci} in the adaptive law are independent of λ_a and λ_b , which only depend on the kernels, the plant parameters, and the coefficients used in the Lyapunov analysis. Choosing γ_{aj} , γ_{bj} , and γ_{ci} to satisfy

$$\max_{i \in \{1, \dots, n\}, j \in \{1, \dots, N\}} \{\gamma_{ci}^2, \gamma_{aj}^2, \gamma_{bj}^2\} := \gamma_0^2 < \frac{\lambda_a}{\lambda_b} \quad (115)$$

we arrive at

$$\dot{V}(t) \leq \frac{-\bar{\lambda}_a}{1 + \Omega} \left(|X(t)|^2 + \hat{\eta}(0, t)^2 + \|\hat{\eta}(\cdot, t)\|^2 \right.$$

$$+ \hat{\alpha}(l(t), t)^2 + \|\hat{\alpha}(\cdot, t)\|^2 \Big) \leq 0 \quad (116)$$

where $\bar{\lambda}_a = \lambda_a - \gamma_0^2 \lambda_b > 0$. Hence, we obtain $V(t) \leq V(0) \forall t \geq 0$. One easily get that $|\tilde{K}(t)|$, $\tilde{d}(t)$, and $\Omega(t)$ are uniformly bounded. Therefore, we obtain that $\|\hat{\eta}(\cdot, t)\|$, $\|\hat{\alpha}(\cdot, t)\|$, and $|X(t)|$ are uniformly bounded. Taking the time derivative of $|X(t)|^2$, $\|\hat{\alpha}(\cdot, t)\|^2$, and $\|\hat{\eta}(\cdot, t)\|^2$ along (75)–(79), we obtain

$$\begin{aligned} \frac{d}{dt} |X(t)|^2 & = 2X^T(t)(A_m X(t) + B \hat{\eta}(0, t) \\ & \quad + B_1 \tilde{d}(t) - B \tilde{K}(t) X(t)) \end{aligned} \quad (117)$$

$$\begin{aligned} \frac{d}{dt} \|\hat{\eta}(\cdot, t)\|^2 & = (q_2(l(t)) + \dot{l}(t)) \hat{\eta}(l(t), t)^2 - q_2(0) \hat{\eta}(0, t)^2 \\ & \quad - \int_0^{l(t)} (q_2'(x) - 2c_4(x)) \hat{\eta}(x, t)^2 dx + 2 \int_0^{l(t)} \hat{\eta}(\cdot, t) \left[\left(\Gamma_t(x, t) \right. \right. \\ & \quad \left. \left. - \int_0^x \check{\vartheta}(x, y) \Gamma_t(y, t) dy - \int_0^x \bar{\vartheta}(x, y) \Gamma_{1t}(y, t) dy \right. \right. \\ & \quad \left. \left. - \int_0^x \hat{N}(x, y; \hat{K}(t)) \left(- \int_0^y \check{\vartheta}(y, z) \Gamma_t(z, t) dz \right. \right. \right. \\ & \quad \left. \left. \left. - \int_0^y \bar{\vartheta}(y, z) \Gamma_{1t}(z, t) dz + \Gamma_t(y, t) \right) dy \right) Z(t) \right. \\ & \quad \left. + \left(D(0; \hat{K}(t)) B \tilde{K}(t) - \dot{\hat{K}}(t) D_{\hat{K}(t)}(x; \hat{K}(t)) \right) X(t) \right. \\ & \quad \left. - \dot{\hat{K}}(t) R(x, t) - D(0; \hat{K}(t)) B_1 \tilde{d}(t) \right] dx \end{aligned} \quad (118)$$

$$\begin{aligned} \frac{d}{dt} \|\hat{\alpha}(\cdot, t)\|^2 & = -(q_1(l(t)) - \dot{l}(t)) \hat{\alpha}(l(t), t)^2 \\ & \quad + q_1(0) \hat{\alpha}(0, t)^2 + \int_0^{l(t)} (q_1'(x) + 2c_1(x)) \hat{\alpha}(x, t)^2 dx \\ & \quad + 2 \int_0^{l(t)} \hat{\alpha}(x, t) \left[-\bar{\lambda}(x, 0) q_1(0) C X(t) + \left(\Gamma_{1t}(x, t) \right. \right. \\ & \quad \left. \left. - \int_0^x \bar{\lambda}(x, y) \Gamma_{1t}(y, t) dy - \int_0^x \check{\lambda}(x, y) \Gamma_t(y, t) dy \right) Z(t) \right] dx. \end{aligned} \quad (119)$$

Recalling the boundedness results of \hat{K} , Γ_t , and Γ_{1t} in (104) and (105) and boundedness of $\dot{l}(t)$ in Assumption 4, according to (78) and (79), we have that $\hat{\eta}(0, t)$ is bounded. The signal $\hat{\alpha}(0, t)$ is also bounded via (76), and then $\hat{\alpha}(l(t), t)$ is bounded through transport PDE (78). Therefore we have that $\frac{d}{dt} |X(t)|^2$, $\frac{d}{dt} \|\hat{\eta}(\cdot, t)\|^2$, and $\frac{d}{dt} \|\hat{\alpha}(\cdot, t)\|^2$ are uniformly bounded according to (117)–(119).

Finally, integrating (116) from 0 to ∞ , it follows that $|X(t)|$, $\|\hat{\alpha}(\cdot, t)\|$, and $\|\hat{\eta}(\cdot, t)\|$ are square integrable. By Barbalat's lemma, $|X(t)|$, $\|\hat{\alpha}(\cdot, t)\|$, and $\|\hat{\eta}(\cdot, t)\|$ tend to zero as $t \rightarrow \infty$.

The achievement of the control objective of adaptively canceling the unmatched disturbance and stabilizing the vibrating string in the output-feedback loop is shown as the following theorem.

Theorem 1: For all initial data $(z(\cdot, 0), w(\cdot, 0)) \in H^1(0, L)$, $X(0) \in \mathbb{R}^n$, $\hat{K}(0) \in \mathbb{R}^{1 \times n}$, $\hat{a}_j(0) \in \mathbb{R}$, and $\hat{b}_j(0) \in \mathbb{R}$, $j = 1, \dots, N$, the output-feedback closed-loop system, including the

plant (1)–(5), the observer (14)–(17), the adaptive update laws (89)–(94), and the control law (98), has the following properties.

- 1) The ODE state $X(t)$ is asymptotically convergent to zero in the sense of $\lim_{t \rightarrow \infty} |X(t)| = 0$.
- 2) The PDE states are uniformly ultimately bounded in the sense of the norm $\|z(\cdot, t)\| + \|w(\cdot, t)\|$.

Proof: Rewriting the observer states in the output-feedback control input (98) as a sum of the plant states and the observer errors according to (12), inserting the result into the plant (1)–(5), through the same steps as in the above state-feedback control designs in Section IV [removing “ \wedge ” for the PDE states in the transformations (42), (43), (58), (59), (73), and (74)], it follows that the target system is a cascade of the observer error dynamics \tilde{z}, \tilde{w} feeding into (α, η, X) dynamics, which are in the form of (75)–(79) (removing “ \wedge ” for the PDE states). For the target system, define a Lyapunov function $\tilde{V}(t)$ in the form of (100) with removing “ \wedge ” for the PDE states, through the Lyapunov analysis similar to the process in the proof of Lemma 2, where the states with “ \wedge ” in adaptive laws (89)–(94) are written as a sum of the states without “ \wedge ” and the observer errors by applying the backstepping transformations (42), (43), (58), (59), and (73), recalling the fact that the observer errors \tilde{z} and \tilde{w} vanish in finite time only depending on the plant parameters according to Lemma 1; the separation principle is verified.

Recalling Lemma 2, property 1) is immediate.

Due to the invertibility and continuity of the backstepping transformations (58), (59), and (73), recalling Lemma 2 and applying the separation principle, we obtain the asymptotic convergence to zero of $\|\hat{v}(\cdot, t)\| + \|\hat{s}(\cdot, t)\|$. According to (42) and (43), we obtain

$$\begin{aligned} & \|\hat{w}(\cdot, t)\|^2 + \|\hat{z}(\cdot, t)\|^2 \\ &= 2\|\hat{v}(\cdot, t)\|^2 + 2N\|\Gamma(\cdot, t)\|^2 + 2\|\hat{s}(\cdot, t)\|^2 + 2N\|\Gamma_1(\cdot, t)\|^2 \\ &\leq 2\|\hat{v}(\cdot, t)\|^2 + 2\|\hat{s}(\cdot, t)\|^2 \\ &\quad + \bar{\gamma}_1 \max_{j \in \{1, \dots, N\}} \{\bar{a}_j^2, \bar{b}_j^2\} + \bar{\gamma}_2 \max_{j \in \{1, \dots, N\}} \{\bar{a}_j^2, \bar{b}_j^2\} \end{aligned} \quad (120)$$

with the positive constants $\bar{\gamma}_1 = 4N^2b_d^2\bar{h}_m^2L$ and $\bar{\gamma}_2 = 4N^2b_d^2p_1^2\bar{h}_m^2L$. Recalling the asymptotic convergence to zero of $\|\hat{v}(\cdot, t)\| + \|\hat{s}(\cdot, t)\|$ and $\bar{\gamma}_1 \max_{j \in \{1, \dots, N\}} \{\bar{a}_j^2, \bar{b}_j^2\}, \bar{\gamma}_2 \max_{j \in \{1, \dots, N\}} \{\bar{a}_j^2, \bar{b}_j^2\}$ being positive constants, we obtain the uniform ultimate boundedness of $\|\hat{w}(\cdot, t)\| + \|\hat{z}(\cdot, t)\|$. Recalling Lemma 1, property 2) is obtained.

The proof is complete.

VII. SIMULATION FOR FLEXIBLE-GUIDE ELEVATOR

A. Model of the Mining Cable Elevator With Flexible Guides

1) *Model and Parameters:* For lateral vibrations, an important factor of influence is the interaction between the cage and the flexible guides. The elastic support of flexible guides is approximated as a spring–damper system, i.e., as a viscoelastic guide [23], [32], where the stiffness and damping coefficients k_c and c_d are not known exactly (see Fig. 2). The wave PDE-modeled lateral vibration dynamics of the mining cable elevator are given by

$$\rho u_{tt} = T(x)u_{xx}(x, t) + T'(x)u_x(x, t) - \bar{c}u_t(x, t) \quad (121)$$

TABLE II
PHYSICAL PARAMETERS OF THE MINING CABLE ELEVATOR

Parameters (units)	values
Initial length L (m)	2000
Final length (m)	200
Cable linear density ρ (kg/m)	8. 1
Total hoisted mass M_c (kg)	15000
Gravitational acceleration g (m/s ²)	9.8
Maximum hoisting velocities \bar{v}_{\max} (m/s)	15
Total hoisting time t_f (s)	150
Cable material damping coefficient \bar{c} (N·s/m)	0.4

$$M_c u_{tt}(0, t) = -k_c u(0, t) - c_d u_t(0, t) + T(0)u_x(0, t) + d(t) \quad (122)$$

$$T(l(t))u_x(l(t), t) = -U(t) \quad (123)$$

where $u(x, t)$ denotes the lateral vibration displacements along the cable shown in Fig. 2, and $x \in [0, l(t)]$ are the positions along the cable in a moving coordinate system associated with the motion $l(t)$, with the origin located at the cage. The function $T(x) = M_c g + x\rho g$ is the static tension along the cable and ρ is the linear density of the cable. The coefficient \bar{c} is the material damping of the cable. The signal $d(t)$ is the uncertain airflow disturbance [31] acting at the cage. The constants k_c and c_d are the unknown equivalent stiffness and damping coefficients of the viscoelastic guide. The modeling process of the lateral vibration dynamics of the mining cable elevator (121)–(123) is based on [7]. The values of the physical parameters of the mining cable elevator tested in the simulation are shown in Table II.

By applying the Riemann transformations $z(x, t) = u_t(x, t) - \sqrt{\frac{T(x)}{\rho}}u_x(x, t), w(x, t) = u_t(x, t) + \sqrt{\frac{T(x)}{\rho}}u_x(x, t)$ and defining $X(t) = [x_1(t), x_2(t)]^T = [u(0, t), u_t(0, t)]^T$, which physically means the lateral displacement and velocity of the cage, (121)–(123) is converted into the 2×2 coupled transported PDE–ODE model given by (1)–(5) with the coefficients defined as

$$q_1(x) = q_2(x) = \sqrt{\frac{T(x)}{\rho}}, c_1(x) = c_3(x) = \frac{-\bar{c}}{2\rho} - \frac{T'(x)}{4\sqrt{\rho T(x)}} \quad (124)$$

$$c_2(x) = c_4(x) = \frac{-\bar{c}}{2\rho} + \frac{T'(x)}{4\sqrt{\rho T(x)}}, p_1 = p_2 = 1 \quad (125)$$

$$A = \begin{bmatrix} 0 & 1 \\ -\frac{k_c}{M_c} & \frac{-c_d - \sqrt{M_c \rho g}}{M_c} \end{bmatrix}, B = \begin{bmatrix} 0 \\ \sqrt{\frac{\rho g}{M_c}} \end{bmatrix} \quad (126)$$

$$B_1 = \begin{bmatrix} 0 \\ \frac{1}{M_c} \end{bmatrix}, C = [0, 2]. \quad (127)$$

The matrices A and B in (126) satisfy Assumption 1. It should be noted that the control input designed based on (1)–(5) with the above coefficients should be multiplied by $-\frac{\sqrt{\rho T(l(t))}}{2}$ in order to convert the input $U(t)$ in (5) into a control force in the practical mining cable elevator, i.e., into the control input $U(t)$ in the boundary condition (123) in the wave PDE model (121)–(123). In the practical mining cable elevator, $l(t)$ is obtained by the product of the radius and the angular displacement of the rotating drum driving the cable, where the angular displacement is measured by the angular displacement sensor at the drum.

2) *Uncertainties:* The unknown damping coefficient and stiffness coefficient (with known bounds) shown in Fig. 2 of the flexible guide are $c_d = 0.4$ and $k_c = 1000$ in (126). The unknown

disturbance $d(t)$ in (1) is modeled as $d(t) = a_1 \cos(\frac{\pi}{8}t) + b_1 \sin(\frac{\pi}{8}t)$, which is a specific case in Assumption 2, where $a_1 = 5$ and $b_1 = 2$ are unknown amplitudes. We assume that we only know their bounds \bar{a}_1 and \bar{b}_1 of 10 and 5 in Assumption 2, respectively.

The target system matrix of the ODE is set as

$$A_m = \begin{pmatrix} 0 & 1 \\ -0.73 & -2.25 \end{pmatrix} \quad (128)$$

whose eigenvalues are -1.8 and -0.4 . According to the unknown system matrix A in (126), the target system matrix A_m in (128), and (10), we know that the (unknown) ideal control parameters k_1 and k_2 are -9 and -30 , respectively. The known bounds of unknown control parameters k_1 and k_2 are set as $[-10, 0]$ and $[-40, 0]$, respectively, considering that the bounds of c_d and k_c in A are known. The parameters $\gamma_{c1}, \gamma_{c2}, \gamma_{a1}$, and γ_{b1} in the adaptive law are chosen as $2, 6.8, 1.2$, and 0.6 , respectively.

3) *Initial Conditions and Moving Boundary*: The initial conditions are given as $w(x, 0) = 0.2 \sin(2\pi x/L)$, $z(x, 0) = 0.3 \sin(3\pi x/L)$, $x_2(0) = 0.5w(0, 0) + 0.5z(0, 0) = 0$, and $x_1(0) = 0$, which satisfies the initial conditions in Theorem 1. The time-varying cable length $l(t)$ is bounded as $0 \leq l(t) \leq L$, where $L = 2000$ m is the maximum length, i.e., Assumption 3 is satisfied. The hoisting velocity curve is shown in [25, Fig. 2]. The maximum velocity of the moving boundary, i.e., maximum hoisting velocity \bar{v}_{\max} given in Table II, satisfies Assumption 4 by recalling $q_1(x)$ and $q_2(x)$ in (124).

B. Numerical Methods

The simulation is conducted based on (1)–(5) with the coefficients (124)–(126). In the simulation program, the closed-loop system on the time-varying domain $[0, l(t)]$ is converted to the one on the fixed domain $[0, 1]$ with time-varying coefficients via introducing a new variable $\ell_1 = x/l(t)$, where the hoisting trajectory $l(t)$ is a predetermined time-varying function, and then, the computation for the plant and observer is conducted using the finite-difference method. The obtained responses are then represented back in the domain $[0, l(t)]$, as shown in this section. The performance of the closed-loop system depends on the step lengths chosen in the finite-difference method. Here, we choose the step sizes of t and ℓ_1 as 0.001 and 0.05 , respectively. The approximate solutions of the kernel PDEs (65)–(72) are also solved by the finite-difference method, where, in addition to $\ell_1 = x/l(t)$ mentioned above, another variable $\ell_2 = y/l(t)$ is introduced, and the lower triangular domain $0 \leq \ell_2 \leq \ell_1 \leq 1$ is discretized as a grid with the uniformed interval of 0.05 . Notice that the derivatives on the left-hand side of (66) and (69) on $x = y$ are represented by a finite-difference scheme in the direction of the information flow, i.e., along the line $x = y$, for the sake of avoiding using the points outside the domain when performing the finite-difference method [3]. The approximate solutions of the kernel PDEs (82)–(85) are obtained with a similar process. For the approximate solutions of the kernel PDEs (28)–(35), the similar process is conducted on the upper triangular domain $0 \leq \ell_1 \leq \ell_2 \leq 1$.

C. Simulation Results

We compare the performance of the proposed controller with a traditional proportional-derivative (PD) controller [19], which is defined as $U_{pd}(t) = -800x_1(t) - 3400x_2(t) - p_2z(l(t), t)$,

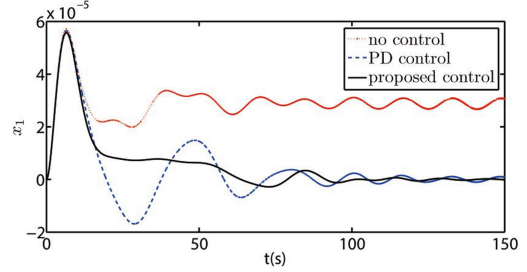


Fig. 3. Responses of $x_1(t)$.

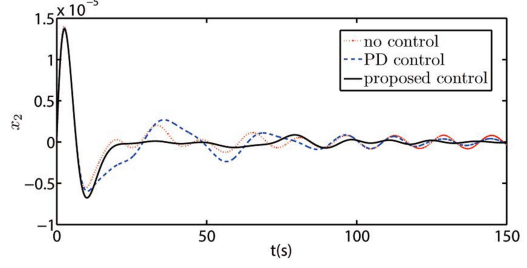


Fig. 4. Responses of $x_2(t)$.

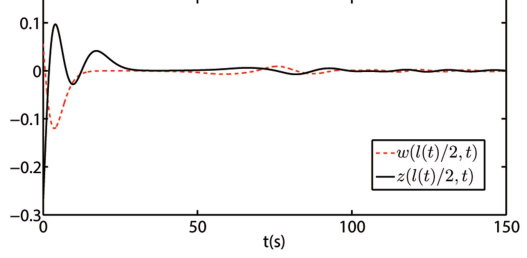


Fig. 5. Responses of PDE states $w(l(t)/2, t)$ and $z(l(t)/2, t)$ under the proposed control.

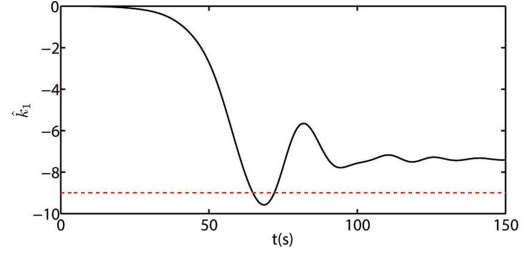


Fig. 6. Self-adjustment of the control parameter \hat{k}_1 to approach the ideal value $k_1 = -9$.

where the design parameters are chosen by trial and error, and the term $-p_2z(l(t), t)$ is to compensate the proximal reflection term in (5) for a fair comparison with the proposed controller. It can be seen in Figs. 3 and 4 that the proposed control guarantees fast reduction of the lateral vibration amplitude and velocity of the cage. Moreover, the proposed controller suppresses the lateral vibration amplitude and velocity of the cage faster than the PD controller. Similar results are observed in the PDE domain, i.e., the closed-loop responses at the midpoint of the spatial domain, shown in Fig. 5.

Figs. 6–9 show that our adaptive laws (89)–(94) can adjust online the control parameters $\hat{k}_1(t)$ and $\hat{k}_2(t)$ to approach the ideal values k_1 and k_2 and estimate the unknown disturbance amplitudes a_1 and b_1 . It is shown that the observer errors of the

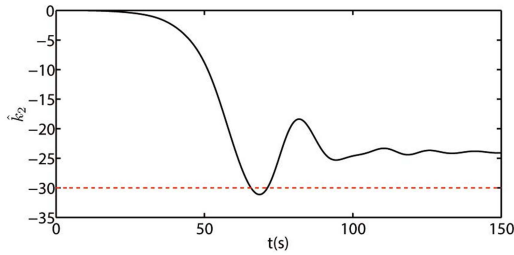


Fig. 7. Self-adjustment of the control parameter \hat{k}_2 to approach the ideal value $k_2 = -30$.

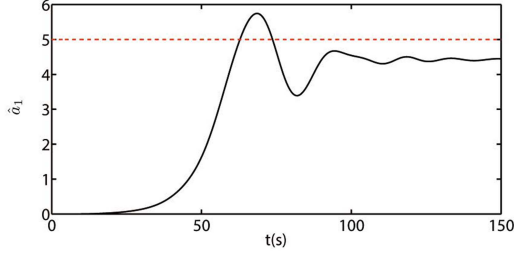


Fig. 8. Estimation \hat{a}_1 of the disturbance amplitude $a_1 = 5$.

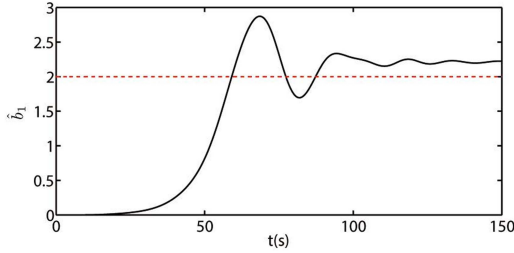


Fig. 9. Estimation \hat{b}_1 of the disturbance amplitude $b_1 = 2$.

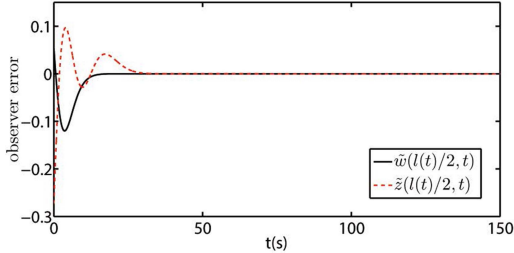


Fig. 10. Responses of observer errors.

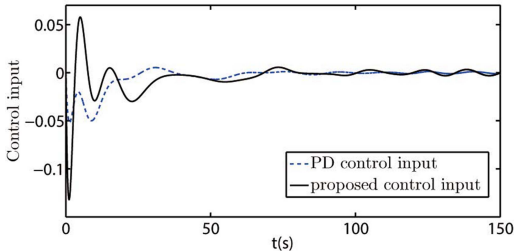


Fig. 11. Control input.

PDE state at the midpoint of the time-varying spatial domain are convergent to zero in Fig. 10. The PD and proposed control inputs applied in (5) are given in Fig. 11. The proposed control input is not completely convergent to zero because the estimates for the harmonic disturbance are not zero in the control law.

VIII. CONCLUSION

In this article, we proposed an adaptive output-feedback boundary control of coupled hyperbolic PDEs with spatially varying coefficients and on a time-varying domain, whose uncontrolled boundary is coupled by a disturbed ODE, where multiple parameters in the state matrix are unknown, and the amplitudes of the harmonic disturbance are unknown as well. The asymptotic convergence to zero of the ODE state and the boundedness of the PDE states were proved via Lyapunov analysis. In numerical simulation, the proposed controller was applied in a mining cable elevator to suppress lateral vibrations during hoisting a disturbed cage moving along a flexible guide.

The proposed design can also be applied in the torsional vibration control of off-shore oil drilling [30] with an uncertain stick-slip instability and disturbances at the bit, anticollocated with the control input at the rotary table on the floating vessel, where active heave compensation [17] is used to isolate the rotary table from the wave-introduced heave motion of the floating vessel.

In future work, the hydraulic actuator dynamics and compensation of signal delay [26] will be incorporated into the control design. The input-to-state stability [20] with respect to the bounds of the disturbances and the situation that unknown parameters also exist in the input matrix B of the ODE will also be considered.

APPENDIX A CALCULATING CONDITIONS OF KERNELS $\bar{\phi}(x, y)$, $\check{\phi}(x, y)$, $\bar{\psi}(x, y)$, AND $\check{\psi}(x, y)$

Substituting (22) and (23) into (19) along (24)–(27), we get

$$\begin{aligned}
 & \tilde{z}_t(x, t) + q_1(x)\tilde{z}_x(x, t) - c_1(x)\tilde{z}(x, t) \\
 & - c_2(x)\tilde{w}(x, t) + \Phi_2(x, t)\tilde{z}(l(t), t) \\
 & = \int_x^{l(t)} [-q_1(x)\bar{\phi}_x(x, y) - c_1(y)\bar{\phi}(x, y) + c_1(x)\bar{\phi}(x, y) \\
 & + c_2(x)\bar{\psi}(x, y) - q_1(y)\bar{\phi}_y(x, y) - q_1'(y)\bar{\phi}(x, y)]\tilde{\alpha}(y, t)dy \\
 & + \int_x^{l(t)} [\check{\phi}_y(x, y)q_2(y) + \check{\phi}(x, y)q_2'(y) - q_1(x)\check{\phi}_x(x, y) \\
 & + (c_1(x) - c_4(y))\check{\phi}(x, y) + c_2(x)\check{\psi}(x, y)]\tilde{\beta}(y, t)dy \\
 & - [l(t)\bar{\phi}(x, l(t)) - \Phi_2(x, t) - q_1(l(t))\bar{\phi}(x, l(t))] \tilde{\alpha}(l(t), t) \\
 & + [\check{\phi}(x, x)(q_2(x) + q_1(x)) - c_2(x)]\tilde{\beta}(x, t) = 0. \quad (A1)
 \end{aligned}$$

Substituting (22) and (23) into (20) along (24)–(27), we obtain

$$\begin{aligned}
 & \tilde{w}_t(x, t) - q_2(x)\tilde{w}_x(x, t) - c_3(x)\tilde{z}(x, t) \\
 & - c_4(x)\tilde{w}(x, t) + \Phi_3(x, t)\tilde{z}(l(t), t) \\
 & = [-c_3(x) - (q_1(x) + q_2(x))\bar{\psi}(x, x)]\tilde{\alpha}(x, t) \\
 & + \int_x^{l(t)} \left(q_2(x)\check{\psi}_x(x, y) + \check{\psi}_y(x, y)q_2(y) + c_3(x)\check{\phi}(x, y) \right. \\
 & \left. + (c_4(x) - c_4(y))\check{\psi}(x, y) + \check{\psi}(x, y)q_2'(y) \right) \tilde{\beta}(y, t)dy \\
 & + \int_x^{l(t)} \left(-q_1(y)\bar{\psi}_y(x, y) + q_2(x)\bar{\psi}_x(x, y) - q_1'(y)\bar{\psi}(x, y) \right. \\
 & \left. + (q_1(x) + q_2(x))\check{\psi}(x, x) \right) \tilde{\alpha}(x, t) = 0.
 \end{aligned}$$

$$\begin{aligned}
& + c_3(x)\bar{\phi}(x, y) + (c_4(x) - c_1(y))\bar{\psi}(x, y) \Big) \tilde{\alpha}(y, t) dy \\
& + \left(\Phi_3(x, t) - \dot{l}(t)\bar{\psi}(x, l(t)) + q_1(l(t))\bar{\psi}(x, l(t)) \right) \tilde{\alpha}(l(t), t) \\
= & 0. \tag{A2}
\end{aligned}$$

Inserting (22) and (23) into (18) and recalling (24), we obtain

$$\begin{aligned}
\tilde{z}(0, t) + p_1 \tilde{w}(0, t) = & - \int_0^{l(t)} (p_1 \bar{\psi}(0, y) + \bar{\phi}(0, y)) \tilde{\alpha}(y, t) dy \\
& - \int_0^{l(t)} (p_1 \check{\psi}(0, y) + \check{\phi}(0, y)) \tilde{\beta}(y, t) dy = 0. \tag{A3}
\end{aligned}$$

For (A1)–(A3) to hold, the conditions of kernels are obtained as (28)–(35).

APPENDIX B

CALCULATING THE CONDITIONS OF KERNELS $\bar{\lambda}(x, y)$, $\check{\lambda}(x, y)$, $\bar{\vartheta}(x, y)$, AND $\check{\vartheta}(x, y)$

Substituting (58) and (59) into (62) along (44)–(48), we obtain

$$\begin{aligned}
& \hat{\alpha}_t(x, t) + q_1(x)\hat{\alpha}_x(x, t) - c_1(x)\hat{\alpha}(x, t) \\
& + \bar{\lambda}(x, 0)q_1(0)CX(t) - \left(\Gamma_{1t}(x, t) - \int_0^x \bar{\lambda}(x, y)\Gamma_{1t}(y, t) dy \right. \\
& \left. - \int_0^x \check{\lambda}(x, y)\Gamma_t(y, t) dy \right) Z(t) \\
= & (\check{\lambda}(x, 0)q_2(0) + \bar{\lambda}(x, 0)q_1(0)p_1) \hat{v}(0, t) \\
& + (c_2(x) - (q_1(x) + q_2(x))\check{\lambda}(x, x)) \hat{v}(x, t) \\
& + \int_0^x \left(\check{\lambda}_y(x, y)q_2(y) + \check{\lambda}(x, y)q_2'(y) - \bar{\lambda}(x, y)c_2(y) \right. \\
& \left. + (c_1(x) - c_4(y))\check{\lambda}(x, y) - q_1(x)\check{\lambda}_x(x, y) \right) \hat{v}(y, t) dy \\
& - \int_0^x \left(\check{\lambda}(x, y)c_3(y) + \bar{\lambda}_y(x, y)q_1(y) + \bar{\lambda}(x, y)q_1'(y) \right. \\
& \left. + \bar{\lambda}(x, y)(c_1(y) - c_1(x)) + q_1(x)\bar{\lambda}_x(x, y) \right) \hat{s}(y, t) dy = 0. \tag{B1}
\end{aligned}$$

Substituting (58) and (59) into (63) along (44)–(48), we obtain

$$\begin{aligned}
& \hat{\beta}_t(x, t) - q_2(x)\hat{\beta}_x(x, t) - c_4(x)\hat{\beta}(x, t) \\
& + \bar{\vartheta}(x, 0)q_1(0)CX(t) + \left(\int_0^x \check{\vartheta}(x, y)\Gamma_t(y, t) dy \right. \\
& \left. + \int_0^x \bar{\vartheta}(x, y)\Gamma_{1t}(y, t) dy - \Gamma_t(x, t) \right) Z(t) \\
= & (c_3(x) + (q_1(x) + q_2(x))\bar{\vartheta}(x, x)) \hat{s}(x, t) \\
& + (\check{\vartheta}(x, 0)q_2(0) + \bar{\vartheta}(x, 0)q_1(0)p_1) \hat{v}(0, t) \\
& + \int_0^x \left(\check{\vartheta}_y(x, y)q_2(y) + \check{\vartheta}(x, y)q_2'(y) - \bar{\vartheta}(x, y)c_2(y) \right. \\
& \left. + q_2(x)\check{\vartheta}_x(x, y) + (c_4(x) - c_4(y))\check{\vartheta}(x, y) \right) \hat{v}(y, t) dy \\
& - \int_0^x \left(\check{\vartheta}(x, y)c_3(y) + \bar{\vartheta}_y(x, y)q_1(y) + \bar{\vartheta}(x, y)q_1'(y) \right)
\end{aligned}$$

$$- q_2(x)\bar{\vartheta}_x(x, y) + \bar{\vartheta}(x, y)(c_1(y) - c_4(x)) \Big) \hat{s}(y, t) dy = 0. \tag{B2}$$

Equations (60) and (61) hold straightforward because of $\hat{\alpha}(0, t) = \hat{s}(0, t)$ and $\hat{\beta}(0, t) = \hat{v}(0, t)$ derived from (58) and (59). Equation (64) is obtained by using (48) and (58). According to (B1) and (B2), the kernels $\bar{\lambda}(x, y)$, $\check{\lambda}(x, y)$, $\bar{\vartheta}(x, y)$, and $\check{\vartheta}(x, y)$ should satisfy (65)–(72).

APPENDIX C

CALCULATING CONDITIONS OF KERNELS $\hat{N}(x, y; \hat{K}(t))$ AND $D(x; \hat{K}(t))$

Inserting (73) at $x = 0$ into (60) and matching with (75)

$$\dot{X}(t) = A_m X(t) - B(K - D(0; \hat{K}(t)))X(t)$$

$$+ B\hat{\eta}(0, t) + B_1\tilde{d}(t)$$

$$= A_m X(t) + B\hat{\eta}(0, t) - B\tilde{K}(t)X(t) + B_1\tilde{d}(t) \tag{C1}$$

we obtain the condition for $D(0; \hat{K}(t))$. Equation (76) holds directly by inserting (73) at $x = 0$ into (61).

Inserting (73) into (78), recalling (75) and (63), we get

$$\begin{aligned}
& \hat{\eta}_t(x, t) - q_2(x)\hat{\eta}_x(x, t) - c_4(x)\hat{\eta}(x, t) \\
& - \left[\Gamma_t(x, t) - \int_0^x \check{\vartheta}(x, y)\Gamma_t(y, t) dy - \int_0^x \bar{\vartheta}(x, y)\Gamma_{1t}(y, t) dy \right. \\
& \left. - \int_0^x \hat{N}(x, y; \hat{K}(t)) \left(- \int_0^y \check{\vartheta}(y, z)\Gamma_t(z, t) dz \right. \right. \\
& \left. \left. - \int_0^y \bar{\vartheta}(y, z)\Gamma_{1t}(z, t) dz + \Gamma_t(y, t) \right) dy \right] Z(t) \\
& - \left(D(x; \hat{K}(t))B\tilde{K}(t) - \dot{\hat{K}}(t)D_{\hat{K}(t)}(x; \hat{K}(t)) \right) X(t) \\
& + \dot{\hat{K}}(t)R(x, t) + D(x; \hat{K}(t))B_1\tilde{d}(t) \\
= & \hat{\beta}_t(x, t) - \int_0^x \hat{N}(x, y; \hat{K}(t))\hat{\beta}_t(y, t) dy - \dot{\hat{K}}(t)R(x, t) \\
& - D(x; \hat{K}(t))\dot{X}(t) - \dot{\hat{K}}(t)D_{\hat{K}(t)}(x; \hat{K}(t))X(t) \\
& - q_2(x)\hat{\beta}_x(x, t) + q_2(x) \int_0^x \hat{N}_x(x, y; \hat{K}(t))\hat{\beta}(y, t) dy \\
& + q_2(x)\hat{N}(x, x; \hat{K}(t))\hat{\beta}(x, t) + q_2(x)D'(x; \hat{K}(t))X(t) \\
& - c_4(x)\hat{\beta}(x, t) + c_4(x) \int_0^x \hat{N}(x, y; \hat{K}(t))\hat{\beta}(y, t) dy \\
& + c_4(x)D(x; \hat{K}(t))X(t) \\
& - \left[\Gamma_t(x, t) - \int_0^x \check{\vartheta}(x, y)\Gamma_t(y, t) dy - \int_0^x \bar{\vartheta}(x, y)\Gamma_{1t}(y, t) dy \right. \\
& \left. - \int_0^x \hat{N}(x, y; \hat{K}(t)) \left(- \int_0^y \check{\vartheta}(y, z)\Gamma_t(z, t) dz \right. \right. \\
& \left. \left. - \int_0^y \bar{\vartheta}(y, z)\Gamma_{1t}(z, t) dz + \Gamma_t(y, t) \right) dy \right] Z(t) \\
& - \left(D(x; \hat{K}(t))B\tilde{K}(t) - \dot{\hat{K}}(t)D_{\hat{K}(t)}(x; \hat{K}(t)) \right) X(t) \\
& + \dot{\hat{K}}(t)R(x, t) + D(x; \hat{K}(t))B_1\tilde{d}(t) \\
= & \left(q_2(0)\hat{N}(x, 0; \hat{K}(t)) - D(x; \hat{K}(t))B \right) \hat{\eta}(0, t)
\end{aligned}$$

$$\begin{aligned}
& - \left(-q_2(x)D'(x; \hat{K}(t)) + D(x; \hat{K}(t))(A_m - c_4(x)) \right. \\
& + \bar{\vartheta}(x, 0)q_1(0)C - \int_0^x \hat{N}(x, y; \hat{K}(t))\bar{\vartheta}(y, 0)q_1(0)Cdy \\
& \left. - q_2(0)\hat{N}(x, 0; \hat{K}(t))D(0; \hat{K}(t)) \right) X(t) \\
& + \int_0^x \left(q_2(y)\hat{N}_y(x, y; \hat{K}(t)) + q_2'(y)\hat{N}(x, y; \hat{K}(t)) \right. \\
& \left. + q_2(x)\hat{N}_x(x, y; \hat{K}(t)) \right) \hat{\beta}(y, t)dy = 0. \tag{C2}
\end{aligned}$$

For (C2) to hold and recalling the condition derived from (C1), conditions of kernels \hat{N} and D are obtained as (82)–(85).

APPENDIX D CALCULATING $\dot{V}(t)$ (102)

Taking the derivative of (101) along (75)–(79), we obtain

$$\begin{aligned}
\dot{V}(t) \leq & \frac{1}{1 + \Omega(t)} \left[-\lambda_{\min}(Q)|X(t)|^2 + 2X^T PB\hat{\eta}(0, t) \right. \\
& + 2X^T PB_1\tilde{d}(t) - 2\tilde{K}(t)X(t)B^T PX(t) \\
& + r_a \int_0^{l(t)} e^{\delta x}\hat{\eta}(x, t) (q_2(x)\hat{\eta}_x(x, t) + c_4(x)\hat{\eta}(x, t)) dx \\
& + r_b \int_0^{l(t)} e^{-\delta x}\hat{\alpha}(x, t) (-q_1(x)\hat{\alpha}_x(x, t) + c_1(x)\hat{\alpha}(x, t)) dx \\
& + \frac{\dot{l}(t)}{2}r_b e^{-\delta l(t)}\hat{\alpha}(l(t), t)^2 - r_a \int_0^{l(t)} e^{\delta x}\hat{\eta}(x, t) \\
& \times \left(D(x; \hat{K}(t))B_1\tilde{d}(t) - D(x; \hat{K}(t))B\tilde{K}(t)X(t) \right) dx \\
& + r_a \int_0^{l(t)} e^{\delta x}\hat{\eta}(x, t) \left(H_b Z(t) - \dot{\tilde{K}}(D_{\hat{K}}X(t) + R(x, t)) \right) dx \\
& + r_b \int_0^{l(t)} e^{-\delta x}\hat{\alpha}(x, t) (H_a Z(t) - \bar{\lambda}(x, 0)q_1(0)CX(t)) dx \\
& \left. + \tilde{K}(t)\Gamma_c^{-1}\dot{\tilde{K}}(t)^T + \sum_{j=1}^N \frac{1}{\gamma_{aj}}\dot{\tilde{a}}_j(t)\tilde{a}_j(t) + \sum_{j=1}^N \frac{1}{\gamma_{bj}}\dot{\tilde{b}}_j(t)\tilde{b}_j(t) \right]
\end{aligned}$$

where

$$\begin{aligned}
H_a = & \Gamma_{1t}(x, t) - \int_0^x \bar{\lambda}(x, y)\Gamma_{1t}(y, t)dy \\
& - \int_0^x \check{\lambda}(x, y)\Gamma_t(y, t)dy \tag{D1}
\end{aligned}$$

$$\begin{aligned}
H_b = & - \int_0^x \check{\vartheta}(x, y)\Gamma_t(y, t)dy - \int_0^x \bar{\vartheta}(x, y)\Gamma_{1t}(y, t)dy \\
& + \Gamma_t(x, t) - \int_0^x \hat{N}(x, y; \hat{K}(t)) \left[- \int_0^y \check{\vartheta}(y, z)\Gamma_t(z, t)dz \right. \\
& \left. - \int_0^y \bar{\vartheta}(y, z)\Gamma_{1t}(z, t)dz + \Gamma_t(y, t) \right] dy. \tag{D2}
\end{aligned}$$

Using integration by parts and $\dot{\tilde{K}}(t) = -\dot{\tilde{K}}(t)$, $\dot{\tilde{a}}_j(t) = -\dot{\tilde{a}}_j(t)$, and $\dot{\tilde{b}}_j(t) = -\dot{\tilde{b}}_j(t)$, recalling (76), applying the Young and Cauchy–Schwarz inequalities, one obtains

$$\dot{V}(t) \leq \frac{1}{1 + \Omega(t)} \left[- \left(\frac{3}{4}\lambda_{\min}(Q) - q_1(0)r_b\bar{d}^2 \right. \right.$$

$$\begin{aligned}
& \left. \left. - \frac{q_1(0)^2}{2}Lr_b\bar{f}^2|C|^2 \right) |X(t)|^2 + \frac{8}{\lambda_{\min}(Q)}|PB|^2\hat{\eta}(0, t)^2 \right. \\
& + 2X^T PB_1\tilde{d}(t) - 2\tilde{K}(t)X(t)B^T PX(t) \\
& - \left(\frac{1}{2}q_2(0)r_a - q_1(0)r_bp_1^2 \right) \hat{\eta}(0, t)^2 \\
& - \left(\frac{1}{2}\delta q_2 r_a - r_a \bar{c}_4 - \frac{1}{2}r_a \bar{q}_2 \right) \int_0^{l(t)} e^{\delta x}\hat{\eta}(x, t)^2 dx \\
& - \frac{1}{2}(q_1 - \dot{l}(t))r_b e^{-\delta L}\hat{\alpha}(l(t), t)^2 \\
& - \left(\frac{1}{2}q_1 \delta r_b - r_b \bar{c}_1 - \frac{1}{2}r_b \bar{q}_1 \right) \int_0^{l(t)} e^{-\delta x}\hat{\alpha}(x, t)^2 dx \\
& + r_a \int_0^{l(t)} e^{\delta x}\hat{\eta}(x, t) \left(H_b Z(t) - \dot{\tilde{K}}(D_{\hat{K}}X(t) + R(x, t)) \right) dx \\
& + r_b \int_0^{l(t)} e^{-\delta x}\hat{\alpha}(x, t) H_a Z(t) dx \\
& - r_a \int_0^{l(t)} e^{\delta x}\hat{\eta}(x, t) \left(D(x; \hat{K}(t))B_1\tilde{d}(t) \right. \\
& \left. - \tilde{K}(t)X(t)B^T D(x; \hat{K}(t))^T \right) dx \left. - \tilde{K}(t)\Gamma_c^{-1}\dot{\tilde{K}}(t)^T \right. \\
& \left. - \sum_{j=1}^N \frac{1}{\gamma_{aj}}\dot{\tilde{a}}_j(t)\tilde{a}_j(t) - \sum_{j=1}^N \frac{1}{\gamma_{bj}}\dot{\tilde{b}}_j(t)\tilde{b}_j(t) \right) \tag{D3}
\end{aligned}$$

where $\bar{f} = \max_{0 \leq x \leq L} \{|\bar{\lambda}(x, 0)|\}$ and $\bar{d} = \max_{(x, \hat{k}_i(t)) \in [0, L] \times [\underline{k}_i, \bar{k}_i]} \{|C - p_1 D(x; \hat{K}(t))|\}$.

From (D3), we arrive at (102).

REFERENCES

- [1] O. M. Aamo, “Disturbance rejection in 2×2 linear hyperbolic systems,” *IEEE Trans. Autom. Control*, vol. 58, no. 5, pp. 1095–1106, May 2013.
- [2] H. Anfinsen and O. M. Aamo, “Disturbance rejection in general heterodirectional 1-D linear hyperbolic systems using collocated sensing and control,” *Automatica*, vol. 76, pp. 230–242, 2017.
- [3] H. Anfinsen and O. M. Aamo, “Adaptive stabilization of 2×2 linear hyperbolic systems with an unknown boundary parameter from collocated sensing and control,” *IEEE Trans. Autom. Control*, vol. 62, no. 12, pp. 6237–6249, Dec. 2017.
- [4] H. Anfinsen and O. M. Aamo, “Adaptive output-feedback stabilization of linear 2×2 hyperbolic systems using anti-collocated sensing and control,” *Syst. Control Lett.*, vol. 104, pp. 86–94, 2017.
- [5] H. Anfinsen and O. M. Aamo, “Adaptive control of linear 2×2 hyperbolic systems,” *Automatica*, vol. 87, pp. 69–82, 2018.
- [6] H. Anfinsen and O. M. Aamo, *Adaptive Control of Hyperbolic PDEs*. New York, NY, USA: Springer, 2019.
- [7] H. Canbolat, D. Dawson, C. Rahn, and S. Nagarkatti, “Adaptive boundary control of out-of-plane cable vibration,” *J. Appl. Mech.*, vol. 65, pp. 963–969, 1998.
- [8] J. M. Coron, R. Vazquez, M. Krstic, and G. Bastin, “Local exponential H^2 stabilization of a 2×2 quasilinear hyperbolic system using backstepping,” *SIAM J. Control Optim.*, vol. 51, no. 3, pp. 2005–2035, 2013.
- [9] J. Deutscher, “Finite-time output regulation for linear 2×2 hyperbolic systems using backstepping,” *Automatica*, vol. 75, pp. 54–62, 2017.
- [10] J. Deutscher, “Output regulation for general linear heterodirectional hyperbolic systems with spatially-varying coefficients,” *Automatica*, vol. 85, pp. 34–42, 2017.
- [11] J. Deutscher, N. Gehring, and R. Kern, “Output feedback control of general linear heterodirectional hyperbolic PDE-ODE systems with spatially-varying coefficients,” *Int. J. Control.*, vol. 92, no. 10, pp. 2274–2290, 2019.
- [12] F. Di Meglio, R. Vazquez, and M. Krstic, “Stabilization of a system of $n + 1$ coupled first-order hyperbolic linear PDEs with a single boundary input,” *IEEE Trans. Autom. Control*, vol. 58, no. 12, pp. 3097–3111, Dec. 2013.

- [13] F. Di Meglio, F. Bribiesca, L. Hu, and M. Krstic, "Stabilization of coupled linear heterodirectional hyperbolic PDE-ODE systems," *Automatica*, vol. 87, pp. 281–289, 2018.
- [14] M. Gugat, "Optimal energy control in finite time by varying the length of the string," *SIAM J. Control Optim.*, vol. 46, pp. 1705–1725, 2007.
- [15] M. Gugat, "Optimal boundary feedback stabilization of a string with moving boundary," *IMA J. Math. Control Inf.*, vol. 25, pp. 111–121, 2007.
- [16] L. Hu, F. Di Meglio, R. Vazquez, and M. Krstic, "Control of homodirectional and general heterodirectional linear coupled hyperbolic PDEs," *IEEE Trans. Autom. Control*, vol. 61, no. 11, pp. 3301–3314, Nov. 2016.
- [17] U. A. Korde, "Active heave compensation on drill-ships in irregular waves," *Ocean Eng.*, vol. 25, no. 7, pp. 541–561, 1998.
- [18] P.-O. Lamare and N. Bekiaris-Liberis, "Control of 2×2 linear hyperbolic systems: Backstepping-based trajectory generation and PI-based tracking," *Syst. Control Lett.*, vol. 86, pp. 24–33, 2015.
- [19] N. Minorsky, "Directional stability of automatically steered bodies," *J. Amer. Soc. Nav. Eng.*, vol. 34, no. 2, pp. 280–309, 1992.
- [20] A. Mironchenko and C. Prieur, "Input-to-state stability of infinite-dimensional systems: Recent results and open questions," *SIAM Rev.*, vol. 62, no. 3, pp. 529–614, 2020.
- [21] L. Su, J. M. Wang, and M. Krstic, "Boundary feedback stabilization of a class of coupled hyperbolic equations with non-local terms," *IEEE Trans. Autom. Control*, vol. 63, no. 8, pp. 2633–2640, Aug. 2018.
- [22] S. Tang and M. Krstic, "Sliding mode control to the stabilization of a linear 2×2 hyperbolic system with boundary input disturbance," in *Proc. Amer. Control Conf.*, Portland, OR, USA, 2014, pp. 1027–1032.
- [23] Y. Terumichi, M. Ohtsuka, and M. Yoshizawa, "Nonstationary vibrations of a string with time-varying length and a mass-spring system attached at the lower end," *Nonlinear Dyn.*, vol. 12, pp. 39–55, 1997.
- [24] R. Vazquez, M. Krstic, and J. M. Coron, "Backstepping boundary stabilization and state estimation of a 2×2 linear hyperbolic system," in *Proc. 50th IEEE Conf. Decis. Control/Eur. Control Conf.*, 2011, pp. 4937–4942.
- [25] J. Wang, S. Koga, Y. Pi, and M. Krstic, "Axial vibration suppression in a PDE model of ascending mining cable elevator," *ASME J. Dyn. Syst., Meas. Control*, vol. 140, 2018, Art. no. 111003.
- [26] J. Wang and M. Krstic, "Delay-compensated control of sandwiched ODE-PDE-ODE hyperbolic systems for oil drilling and disaster relief," *Automatica*, vol. 120, 2020, Art. no. 109131.
- [27] J. Wang and M. Krstic, "Vibration suppression for coupled wave PDEs in deep-sea construction," *IEEE Trans. Control Syst. Technol.*, vol. 29, no. 4, pp. 1733–1749, Jul. 2021.
- [28] J. Wang and M. Krstic, "Output-feedback control of an extended class of sandwiched hyperbolic PDE-ODE systems," *IEEE Trans. Autom. Control*, vol. 66, no. 6, pp. 2588–2603, Jun. 2021.
- [29] J. Wang, Y. Pi, and M. Krstic, "Balancing and suppression of oscillations of tension and cage in dual-cable mining elevators," *Automatica*, vol. 98, pp. 223–238, 2018.
- [30] J. Wang, S.-X. Tang, and M. Krstic, "Adaptive output-feedback control of torsional vibration in off-shore rotary oil drilling systems," *Automatica*, vol. 111, 2020, Art. no. 108640.
- [31] J. Wang, S.-X. Tang, Y. Pi, and M. Krstic, "Exponential anti-collocated regulation of the disturbed cage in a wave PDE-modeled ascending cable elevator," *Automatica*, vol. 95, pp. 122–136, 2018.
- [32] W. D. Zhu and G. Y. Xu, "Vibration of elevator cables with small bending stiffness," *J. Sound Vib.*, vol. 263, pp. 679–699, 2003.



Ji Wang (Member, IEEE) received the Ph.D. degree in mechanical engineering from Chongqing University, Chongqing, China, in 2018.

From 2019 to 2021, he was a Postdoctoral Scholar with the Department of Mechanical and Aerospace Engineering, University of California, San Diego, La Jolla, CA, USA. He is currently an Associate Professor with the Department of Automation, Xiamen University, Xiamen, China.

His research interests include modeling and control of distributed parameter systems, active disturbance rejection control, event-triggered control, and adaptive control, with applications in cable-driven mechanisms.

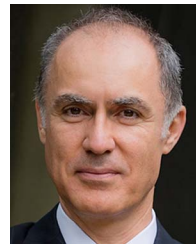
Dr. Wang has been an Associate Editor for *Systems and Control Letters* since 2021.



Shu-Xia Tang (Senior Member, IEEE) received the Ph.D. degree in mechanical engineering from the Department of Mechanical and Aerospace Engineering, University of California, San Diego, La Jolla, CA, USA, in 2016.

She is currently an Assistant Professor with the Department of Mechanical Engineering, Texas Tech University, Lubbock, TX, USA. Her research interests include stability analysis, estimation, and control design of distributed parameter systems.

Dr. Tang is an Associate Editor for *Journal of Control, Automation and Electrical Systems* and an Editorial Board Member of the IEEE Control Systems Society and ASME Dynamic Systems and Control Division. She is a Member of the Technical Committee on Distributed Parameter Systems of the IEEE Control Systems Society.



Miroslav Krstic (Fellow, IEEE) received the degree (summa cum laude) in electrical engineering from the Department of Electrical Engineering, University of Belgrade, Yugoslavia, in 1989, and the M.S. and Ph.D. degrees from the Department of Electrical and Computer Engineering, University of California, Santa Barbara, CA, USA, in 1992, and 1994, respectively.

He is currently a Distinguished Professor of Mechanical and Aerospace Engineering with the University of California, San Diego (UCSD), La Jolla, CA, USA, where he holds the Alspach endowed chair and is the Founding Director of the Cymer Center for Control Systems and Dynamics. He is also the Senior Associate Vice-Chancellor for Research with UCSD. He has coauthored 15 books on adaptive, nonlinear, and stochastic control, extremum seeking, control of partial differential equation systems, including turbulent flows and control of delay systems.

Prof. Krstic is the recipient of the University of California Santa Barbara Best Dissertation Award and Student best paper awards at IEEE Conference on Decision and Control and American Control Conference. He is a Fellow of the International Federation of Automatic Control (IFAC), the American Society of Mechanical Engineers (ASME), the Society for Industrial and Applied Mathematics (SIAM), the American Association for the Advancement of Science, and the Institution of Engineering and Technology (U.K.), an Associate Fellow of the American Institute of Aeronautics and Astronautics, and a foreign member of the Serbian Academy of Sciences and Arts and the Academy of Engineering of Serbia. He is also the recipient of the Richard E. Bellman Control Heritage Award, the SIAM Reid Prize, the ASME Oldenburger Medal, the Nyquist Lecture Prize, the Paynter Outstanding Investigator Award, the Ragazzini Education Award, the IFAC Nonlinear Control Systems Award, the Chestnut Textbook Prize, the Control Systems Society Distinguished Member Award, the Presidential Early Career Award for Scientists and Engineers, National Science Foundation CAREER Award, and Office of Naval Research Young Investigator awards, the Schuck (1996 and 2019) and Axelby Paper Prizes, and the first UCSD Research Award given to an engineer. He has also been awarded the Springer Visiting Professorship at the University of California Berkeley, the Distinguished Visiting Fellowship of the Royal Academy of Engineering, the Invitation Fellowship of the Japan Society for the Promotion of Science, and four honorary professorships outside of the United States. He is the Editor-in-Chief for *Systems and Control Letters*, a Senior Editor for *Automatica* and *IEEE TRANSACTIONS ON AUTOMATIC CONTROL*, and an Editor for two Springer book series. He has served as the Vice-President for Technical Activities of the IEEE Control Systems Society (CSS) and as the Chair of the IEEE CSS Fellow Committee.